The dynamics of glacial till erosion:

hydraulic flume tests on samples from Medway Creek, London, ON

Leila Pike

Thesis

Department of Civil Engineering and Applied Mechanics

McGill University, Montreal

December, 2014

A thesis submitted to McGill University in partial fulfillment

of the requirements of the degree of Master of Civil Engineering.

Abstract

The erosion of till material from the river bank of Medway Creek in London, Ontario was studied to determine the erosion mechanisms and critical shear stress of the till, and to understand how the alluvial cover, particularly the gravel particles, impacts the erosion process. Samples were collected from Medway Creek and were tested under a unidirectional current in a hydraulic flume at McGill University under a unidirectional current. Samples were tested under three separate sets of conditions: samples at their natural moisture content in clear flow conditions, air-dried samples in clear flow conditions, and samples at their natural moisture content with large gravel particles present in the flume. The two latter tests were performed to determine any effects that weathering and the presence of alluvial material may have in the erosion process. The results show that mass erosion was the dominant form of erosion, occurring around natural planes of weakness and irregularities, such as gravel particles, within the material. The critical shear stress was observed to be approximately 8 Pa. The effect of drying on the erosion process was extreme – the critical shear stress dropped to below 1 Pa and the structure of the cohesive material disintegrated. The presence of gravel particles led to increased surface erosion due to impacts and a more rapid progression of the erosion. In summary, the till erodes around planes of weakness and irregularities, till exposed to a wetting-drying is most at-risk of erosion, and the presence of gravel does not provide a protective layer over the till and instead lowers the critical shear stress.

Résumé

L’érosion des berges en tillite du ruisseau Medway à London, Ontario, a été étudiée afin de déterminer le mécanisme d’érosion de la tillite, la valeur de la contrainte de cisaillement critique, et pour comprendre comment la couverture alluviale, en particulier les graviers, impacte le processus d’érosion. Des échantillons ont été prélevés dans le ruisseau Medway et testés dans un canal hydraulique à l’Université de McGill, sous un courant unidirectionnel. Les échantillons ont été testés avec trois ensembles de paramètres distincts : les échantillons étant à leur taux d’humidité naturel sous un écoulement d’eau claire, les échantillons ayant été préalablement séchés à l’air puis soumis à un écoulement d’eau claire et les échantillons étant à leur taux d’humidité naturel avec de grosses particules de gravier présentes dans le canal. Les deux dernières expériences ont été effectuées afin de déterminer les effets des conditions météorologiques et de la présence d’alluvions sur le processus d’érosion. Les résultats ont montré que l’érosion par blocs est la forme d’érosion dominante, se produisant autour des failles naturelles et des irrégularités de la structure, telles que les graviers. La contrainte de cisaillement critique a été obtenue autour de 8 Pa. L’effet du séchage est extrême : la contrainte de cisaillement critique descend dans ce cas en-dessous de 1 Pa et la structure du matériau perd sa cohérence et se désagrège. La présence de graviers mène à un plus fort abaissement de la surface du sol, du fait des impacts, et à une progression plus rapide de l’érosion. En conclusion, la tillite s’érode à proximité des failles et des irrégularités, une tillite exposée à un cycle de mouillage-séchage risque davantage d’être érodée, et la présence de graviers ne constitue pas une couche protectrice pour la tillite mais au contraire abaisse la valeur de la contrainte de cisaillement critique.

Acknowledgements

I would like to thank both of my supervisors, Professor Susan Gaskin and Professor Peter Ashmore, for providing me with guidance for the past two years and for reading and re-reading my thesis countless times. I would especially like to thank Professor Gaskin for taking me on as a student, teaching me about water resources and hydrology, and giving me invaluable knowledge on water use in the world. I am thankful for the knowledge on Medway Creek that Professor Ashmore shared with me, his recommendations for past research to look into, and for his help carrying samples out of the river.

There are many people at Western University who volunteered their time to help me collect samples of till from Medway Creek: Sarah Peirce, who helped me carry samples; Nati Bergman, who went into the river to get submerged samples, helped me lug samples, and shared with me his research on the river; and James Thayer, who put in a long day helping me carry the heaviest of the samples out of the river. Without help from these people, I would not have had adequate samples to perform my tests.

I am utterly grateful for John Bartczak and his never-ending help when it came to repairing the flume. John not only helped me assemble the flume, but he helped me brainstorm my testing, cut my samples, and show me how to use the flume. Without John, I would not have been able to get the flume running.

Lastly, I'd like to thank Tom Nosal for helping me run the flume tests when I needed an extra hand, helping me and John assemble the flume, and for providing support and feedback regarding my presentation and thesis.

Table of Contents

List of Figures:

List of Tables:

Notation

D_{50} Diameter at which 50% of a sample's mass is comprised of smaller particles

τ shear stress

γ_w specific weight of water

S slope

R hydraulic radius

1.0 Introduction

1.1 Topic Overview

Erosion of river bed and banks, as well as channel incision, are natural processes but they can disrupt the surrounding built environment and infrastructure. While the process of a river eroding, changing course, and meandering, is a natural phenomenon, its rate of erosion may be increased by, for example, increases in stream discharge and peak flows following urbanization, or by climate change bringing a higher frequency and intensity of storm events (Kundzewicz and Takeuchi 1999). Unfortunately, with the existence of extensive human infrastructure near watercourses, erosion cannot be ignored. Structurally-engineered methods to mitigate the process, such as levees, dams, river diversions, bank and bed protection, and channelization, can have adverse effects on the environment and do not guarantee a long-term solution (Goulter and Myska 1987). An alternative is to better understand the processes to aid in the prediction and prevention of unwanted natural consequences due to human presence or to design interventions that retain as much natural functioning of the system as possible.

In glaciated landscapes as in southern Ontario, many rivers are incised into glacial deposits such as till. Much of southern Ontario is underlain by Quaternary glacial deposits formed during the Wisconsin glaciation that consist of gravelly till and lacustrine deposits such as silts, sands, and clays (Chapman and Putnam 1973). Lodgement till is deposited by “plastering” from the sliding base of the glacier and produces massive diamiction (sediment of mixed sizes) with shear and pressure discontinuities. The overlying glaciers that created the till exerted high pressures, overconsolidating the material and giving the till high bulk densities and shear strength, to the extent that the material is often treated as soft bedrock (Dreimanis 1976; Davidson-Arnott and

Langham 2000; Mier and Garcia 2011). While till is a cohesive material, it differs from clay because it is an unsorted sediment with a wide range of particle sizes, from clay sizes to gravel particles to large boulders, embedded within it. Adding to the complexity of rivers incised in till is the presence of alluvial material (non-cohesive sand and gravel originating from the till and other glacial deposits) partially and/or intermittently covering the till river beds. The combination of the cohesive nature of the till and the semi-alluvial nature of the rivers has led to difficulty in establishing erosion criteria, rates, and predictions for till rivers in southern Ontario.

The erosion of till rivers is a complex process due to the cohesive nature of the till, the internal structure of the material, and the semi-alluvial behavior of the river. While intermittently covered by alluvial material, the till may be exposed in both the bed and the banks of a river. The cohesive nature of the till is similar to that of clay and results in erosion processes similar to those found in clay-bed rivers. Clay has been observed to erode by mass erosion (in chunks) rather than on a particle-by-particle basis, as is seen in non-cohesive sediments, but it can also erode through the breakage of inter-particle bonds and by the liquidation of fluid mud in estuarine environments. The semi-alluvial nature of the rivers is due to the embedded gravel particles within the till eroding out of the till and becoming a partial and/or intermittent alluvial cover over the bed. For geomorphic and engineering assessments, it is important to determine the critical shear stress of the till and compare it with that of other cohesive materials. The influence of the semi-alluvial nature of the till on the erosion processes and on the critical shear stress also needs to be studied.

The erosion of cohesive material is hard to quantify and difficult to study. Unlike the erosion and transport of non-cohesive alluvium which is relatively well-understood (Raudkivi 1998), river channels formed in non-alluvial, cohesive boundary material (such as bedrock, clay and some glacial till deposits) and the processes of erosion of such material are not well-understood or predictable, and methods of testing erodibility are not yet standardized. The variety of in-situ and laboratory testing methods and procedures that have been used produce results that are difficult to compare and little is known about fundamental parameters such as the critical hydraulic conditions for initiating erosion or even the actual mechanisms of erosion. No fluvial erosion study on till has yet incorporated the semi-alluvial aspect of the rivers.

The semi-alluvial nature of till rivers has only recently been acknowledged and could have a large role in the erosion of the material. The term “semi-alluvial” was introduced to describe rivers incised into glacial deposits which have a high resistance to erosion, but are also sensitive to streamflow change, so that the adjustability to discharge and sediment supply falls between that of non-cohesive alluvial river beds, and hard non-alluvial bedrock streams that are the least sensitive to flow regime changes. The definition also includes the intermittent alluvial covering present on till beds (Turowski 2012; Meshkova 2012; Hrytsak 2012). The alluvial covering, especially the gravel and coarse grains, could be an important agent of the erosion process by both protecting the underlying till from erosion and by contributing to erosion by abrasion and impacts to the surface from the moving particles, which is known to be important for hard rock (Sklar and Dietrich 2004, Johnson and Whipple 2007, and Chatanantavet and Parker 2008).

A better understanding of the geomorphology of rivers can help prevent unwanted harm to infrastructure from river erosion and allow scientists to accurately model the changing fluvial landscape. Traditional structurally-engineered methods to control the paths of rivers do not provide long-term protection. A better method is to increase the understanding of when and why rivers erode and then design protection methods that retain the natural functioning of the system. Increasing the knowledge of till river geomorphology will also allow scientists and researchers to model the changing landscape and more accurately research and study future river conditions.

The critical shear stress of the bed and bank material in a river is information that can be used to help predict river channel erosion, as well as design channels or remediate erosion, especially with changing flow conditions. Urbanization can cause an increase in stream discharge and climate change brings a risk of higher frequencies and intensities of storms, both of which can raise peak flows. Changing flow conditions, and especially an increase in peak flows, can cause more channel widening and erosion. Knowing the main mechanisms of erosion and the critical shear stress for erosion of the material will allow for better design in erosion prevention and remediation endeavors.

1.2 Research Objectives

The subject of this research was to increase understanding of the erosional resistance and mechanisms of erosion of till samples from a river in southern Ontario. Few previous tests have involved the real processes of erosion while also testing intact samples under shear stress conditions similar to those in the river. This study estimated, using laboratory flume tests, the critical shear stress of the cohesive till material, or the shear stress required to initiate erosion. According to past research (addressed in Section 2.0), this value could lie between < 1 Pa and 20 Pa. There were two main goals of the study. The first was to observe the mechanism of till erosion and estimate the critical bed shear stress for the initiation of erosion. Experiments were carried out in a hydraulic flume, as opposed to *in situ,* in order to have a greater measure of experimental control, and better determine the critical shear stress. The second goal was to understand how the alluvial cover, particularly the gravel particles, impacts the erosion process.

2.0 Literature review: Till and Erosion

2.1 Semi-Alluvial Channels

The term ‘semi-alluvial’ in relation to river channel typology is relatively recent and not widely used, but has allowed for more depth in defining the behavior and classification of river types and boundary material. Defined loosely by Meshkova et al. (2012) as ‘river sections that have a solid boundary other than natural hard bedrock,’ semi-alluvial channels fall between the range of behaviour of bedrock and alluvial channels. The development of the use of the term is important in furthering the understanding of the morphology of a river and its processes beyond those of strictly bedrock or of strictly alluvial nature. For instance, cohesive boundaries, such as marine or lacustrine clays, are able to constrain and confine rivers, a long-time defining characteristic of bedrock rivers (Turowski et al. 2008). Semi-alluvial channels with cohesive boundaries are shown schematically in Figure 1. However, the boundary types do not need to be limited to fully alluvial or fully cohesive as seen in Figure 1 – they can be partially alluvial or partially cohesive as well.

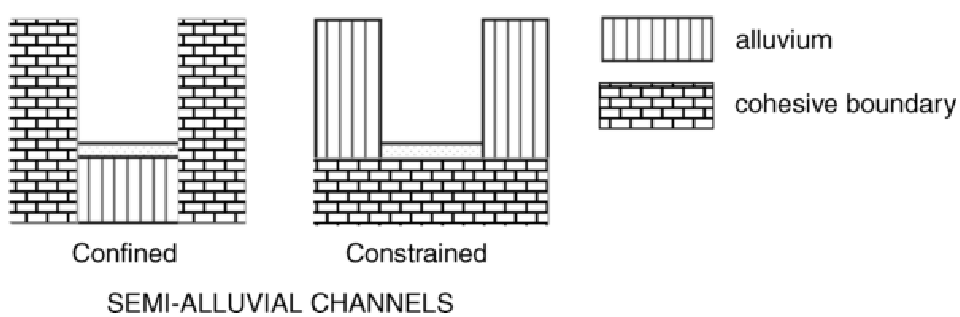

Figure 1: Semi-alluvial channel types (Meshkova et al. 2012)

Many rivers in Canada, and especially till rivers, fall under the classification of semi-alluvial rivers (Ashmore and Church 2001). Till is not an alluvial material and does not readily erode as such. However, it does produce a steady supply of alluvial material, as finer particles are eroded and carried downstream in suspension, that intermittently covers the surface of the till, thus falling outside the realm of classic definitions of bedrock channels (Foster 1998, Tinkler and Wohl 1998). Hrytsak (2012) observed that the characteristics of till rivers in southern Ontario, including the confining banks and stable, but not widespread, alluvial cover, to be distinct from those of alluvial and bedrock channels and to be better defined as semi-alluvial channels. A study by Ashmore and Church (2001) expressed a concern with the impression of stability that semi-alluvial rivers give. The rivers are constrained and exhibit minimal erosion during normal flows, but during high flows or flood events, the shear stresses applied to the material may exceed the threshold for erosion, and the rivers may become much more sensitive to flow changes. The designers of engineering works and erosion protection need to be wary of the seemingly-stable state of these rivers and provide energy dissipation measures to reduce the shear stresses applied to the bed and banks of rivers during high flow events.

2.2 Erosion Mechanisms

The erosion of cohesive sediments of river beds and banks is not well understood. Non-cohesive erosion can be quantified and calculated using first principles and physics (equations of continuity, momentum and energy), since it occurs once the lift and drag forces become greater than the weight of the particle and the frictional resistance of the surrounding particles (Raudkivi 1998). Non-cohesive erosion processes occur for particle sizes above 60 μm. Once the particle sizes become smaller than 60 μm, they begin to form electro-chemical bonds, e.g. Van der Waals forces, and the material becomes cohesive (Mehta et al. 1989). As a general rule, the smaller the particle, the more cohesive it becomes. Silt particles range from 2 and 60 μm, and clay particles are less than 2 μm. Clay exhibits a more cohesive behavior, mainly because the particles are thin and plate-like, which encourages inter-particle bonds due to a high surface area to volume ratio

(Terzaghi 1942). Due to their small size, the erosion of cohesive sediments cannot be analyzed on an individual particle basis, and alternate approaches are used, although no standard method has been widely accepted. The difficulty in studying cohesive sediment erosion goes beyond the cohesive bonds in the sediment to also include an uncertainty over whether analysis of individual particles is relevant, the added complication of abrasion processes, and a variety of specific *in situ* conditions that may have varying effects on the initiation and rate of erosion, such as the presence of waves, freezing and thawing cycles, alluvial cover, the history of deposition, and chemical composition of the material. Studying individual cases is presently the only way to determine the erosion characteristics of cohesive sediments for a particular river (Mier and Garcia 2011).

Cohesive erosion has been described as due to three mechanisms: surface erosion, bulk erosion, and/or entrainment of fluid mud (Krone 1999; Mehta et al. 1989). Surface erosion occurs once the inter-particle bonds are broken between particles near the surface, due to the application of a shear stress causing hydrodynamic lift and drag forces. It is often described as a smoothing or pitting of the surface (Krone 1999). For till, surface erosion of the particles can reveal embedded gravel in the till (Mier and Garcia 2011). In high flow conditions, surface erosion is the mechanism that occurs enhanced by the movement and relocation of the alluvial cover, which create conditions with high abrasion potential due to sand and gravel particles saltating downstream (Mier and Garcia 2011; Kamphuis and Hall 1983; Chatanantavet and Parker 2009).

Bulk erosion, or mass erosion, is described as the breaking off of chunks of sediment at irregularities or planes of weakness in the sediment structure, and has proved to be the most dominant form of erosion for cohesive material (Krone 1999). Lefebvre et al. (1985) outlined the importance of the "structuration" of the sediment, or the skeleton that bonds the particles together, since it is the flaws in the skeleton, which delineate the pieces that erode due to bulk erosion. Bulk erosion of cohesive material has been observed in multiple studies. Kamphuis et al. (1990) tested till from Dingman Creek in London, Ontario in a laboratory flume and found that the erosion process occurred in blocks around gravel particles and disturbances in the sediment. Even with no gravel present, erosion occurred by spalling of blocks and flakes. A flume study on till from the St. Clair River (Ontario-Michigan) by Mier and Garcia (2011) found the initial erosion to occur by the peeling of layers of cohesive sediments, as well as the breaking of chunks of sediment which saltated downstream. A flume study on Champlain Sea Clay by Gaskin et al. (2003) outlined the process of mass erosion to occur first by the formation of cracks and fissures, which then outlined blocks in the clay structure, which proceeded to erode by breaking off into chunks. Lefebvre et al. (1985) performed drill hole tests on clay from Eastern Canada and determined erosion to occur by the pulling out of larger particles, chunks, or aggregates, at areas with heterogeneities or defects. Each of these studies also noted that the failure of bonds does not seem significant in the erosion process compared to the pulling out of blocks of the sediment.

Entrainment of fluid mud occurs in deposits with high water content, particularly freshly deposited sediment in estuaries. The fluid mud will mix with the overlying flow due to the high moisture content and low density. The suspension density decreases with the progress of erosion, and as the flow velocity increases, the rate of entrainment will also increase (Mehta et al. 1989). Entrainment of fluid mud is not relevant to this particular study, and so the research will focus on the other two mechanisms.

This study will determine if mass erosion is the predominant form of erosion in till, as past literature suggests. Since the erosion mechanism is part of the research question, it is important for the testing method used in this research to allow for the mechanism of both mass erosion and surface erosion to occur, to understand which is dominant and the relationship, if any, between the two.

2.3 Abrasion

Abrasion is the process of wearing away the surface of material due to friction. In rivers, this occurs when saltating or suspended sand or gravel particles impact the bed of the river, causing the river bed material to erode. The presence of sand or gravel particles in the water column has been shown to decrease the critical shear stress of a sample due to abrasion of the sediment (Kamphuis 1983 and Kamphuis et al. 1990). Sand is seen to have the largest effect on erosion when it undergoes saltation or milling, causing a lengthening, widening, and deepening of any imperfections in the clay material due to sand blasting (Kamphuis 1983). The presence of sand has also been seen to increase the amount of erosion occurring, increasing erosion rate by up to five times (Kamphuis et al. 1990). The erosion by the sand suspension was initiated by the movement of the sand particles, with the critical shear stress being between 0 and 2 Pa, which corresponds to the shear stress required to start movement of the sand particles. This led Kamphuis et al. (1990) to propose that, in situations where the eroding water can contain solid particles, the erosion of cohesive soils might be controlled by the size of those particles. Recent research on fluvial abrasion of bedrock has elaborated this idea. The flow and particle velocity also affects the frequency of impact with the bed and the size of the most effective abrading particle increases as flow velocity increases. However, there is an upper limit to the rate at which abrasion can erode the material because increasing shear stress values will reduce the frequency of the bed load impacts as the particles become suspended (Sklar and Dietrich 2004). If abrasion particles, such as gravel pieces, come from the eroded till material, then the particle size distribution of the till is important in understanding the size of the abrasion particles and any potential for abrasion. The past studies by Kamphuis (1983) and Kamphuis et al. (1990) focused on abrasion due to sand particles. However, many till-bed rivers have predominantly gravel particles on the channel bed. Therefore, it is not necessarily abrasion that occurs, but rather the impact of large gravel particles that may cause erosion. More research will need to be performed on this aspect to understand the nature of particle impacts and abrasion that are most relevant to till rivers.

2.4 Alluvial Cover

The relationship between the alluvial cover, sediment supply, and erosion of gravel till rivers is complex, and has seldom been studied. It is generally understood that an alluvial cover will develop in a river when the sediment supply to the river channel reach is higher than the transport capacity, however there are often more factors involved, such as grain size and bed roughness (Johnson and Whipple 2007). An alluvial cover is common in bedrock rivers, and an overview of these studies is provided below because they provide some possible insights applicable to semi-alluvial channels.

Past research on the alluvial cover in bedrock rivers has examined fluvial incision into bedrock with a particular focus on the movement and settlement of the alluvial cover (Sklar and Dietrich 2004, Johnson and Whipple 2007, and Chatanantavet and Parker 2008). There is some agreement that bed roughness and/or topography, grain size, and sediment supply are the main factors that determine whether an alluvial cover will develop and the extent to which the alluvial material will cause or inhibit incision into bedrock, although the importance of each parameter is open to discussion. Sklar and Dietrich (2004) concluded that the main difference between sediment causing erosion and sediment preventing erosion is related to the sediment supply, with maximum erosion occurring at a moderate sediment supply relative to the sediment transport capacity, since at a low sediment supply there will be minimal abrasion, and at a high sediment supply an alluvial cover will develop, thus protecting the underlying material. This is often referred to as the "tools and cover" effect. The study concluded that grain size was one of the most important factors controlling bedrock incision rates, with a larger grain size leading to increased incision, and the most abrasive particles being those which saltate along the bed at high velocities. However, the more recent research by Johnson and Whipple (2007) and Chatanantavet and Parker (2008) found that the importance of sediment supply with regards to alluvial cover and abrasion is not as important as other factors, such as topography and bed roughness. Johnson and Whipple (2007) created varying topographies in their flume studies and found that potholes and local lows in the surface were most susceptible to incision, with low areas causing an increase in local sediment flux. However, this also caused gravel to deposit in the lows and inhibit further abrasion. Overall, the study found that once the material underwent erosion or areas of relief appeared, bed topography was the leading control on sediment impact location and intensity. Similarly, Chatanantavet and Parker (2008) found that bed roughness was the leading parameter in whether the alluvial cover would settle in a particular location. While this may be true in hard bedrock rivers, a study by Hrytsak (2012) on the alluvial cover in semi-alluvial rivers with a till substrate concluded that till is too soft of a material to form topography that would encourage deposition, so the bed roughness and topography may be irrelevant in till rivers, in which case other controlling factors need to be studied. It needs to be determined whether abrasion occurs in till-beds and whether coarse gravel deposits "protect" the bed from erosion.

One of the main differences between bedrock rivers and till rivers in terms of the presence of alluvial material, is the ability for till rivers to provide their own sediment supply. Large sand and gravel particles embedded within the till material can become part of the alluvial cover (if present) when eroded. However, the contribution to the alluvial cover from embedded particles is not straight-forward. Mier and Garcia (2011) performed erosion studies on till material without specifically looking at the alluvial cover, and noted in their studies that as gravel particles within the till were uncovered, the surrounding cohesive material kept them in place, even though they would have been transported at the applied shear stress implemented. In this sense, perhaps in till rivers it is the cohesion, rather than the bed roughness or topography, that determines where an alluvial cover will form and that prevents the cover from moving.

The differences between bedrock rivers and till rivers with regards to the behavior of alluvial material is significant enough to question the relevance of the previous bedrock studies. Since past studies on cohesive materials have determined that the natural structure of the material itself is important in understanding the erosion mechanisms and processes, the synthetic bedrock material used in previous studies may behave in an entirely different manner. Past literature suggests that till erodes similarly to clay in the form of mass erosion, and not by the creation of grooves and valleys in the bed as the bedrock studies have shown, so not only will erosion occur differently in till rivers, but the deposition of the alluvial material may not follow the same patterns. Lastly, the cohesive nature of the till material may have an important and deciding role in when and where the alluvial cover will form. Further studies on the complex relationship between the gravel particles embedded within the till, the erosion of the till material, and the formation and movement of the alluvial cover, are required to get a better understanding of the role the alluvial material has on the erosion and geomorphology of till rivers.

2.5 Additional Factors Influencing Erosion

There are many additional factors that are also studied for their effects on erosion, including the properties of the sediment, vegetation, and weathering. These features are commonly isolated within each experiment; however, combinations of these elements are usually present *in situ*, thus adding to the difficulty of studying erosion processes and rates. The following sections provide an overview of how the properties of sediment, presence of vegetation, and weathering effect the erosion of cohesive materials.

2.5.1 Properties of Sediment

Material properties such as average particle size, particle size distribution, bulk density, and water content are sometimes used to predict erosion in lieu of being able to use first principles and physics (energy and momentum), due to the bonds present between particles. Some researchers believe these properties to be important and influential in determining the erodibility of cohesive sediment (Govers and Loch 1992; Krishnappan and Droppo 2006; Grabowski et al. 2011; Mier and Garcia 2011). However, other researchers, such as Kamphuis et al. (1990), have determined there to be no definite relationship between the critical shear stress, or the amount of erosion, and any of the bulk soil parameters. Nevertheless, the properties are further explored in terms of potential impacts on erosion.

2.5.1.1 Particle Size

The correlation between particle size and erosion threshold is not straightforward for cohesive sediments. A positive correlation has been found between the erosion threshold and particle size for non-cohesive sediments due to the greater mass of the larger particles. However, for cohesive materials, once the average particle size drops into the fines range, the particles become bonded and this correlation is no longer valid (Grabowski et al. 2011; Mier and Garcia 2011). For materials that have low clay contents, but before they are considered cohesive, clay particles can fill the voids between the sand particles, creating a smoother surface which makes the material more difficult to erode. At this point, studies have found a negative correlation between critical shear stress and sand content (Grabowski et al. 2011). The material will become cohesive with an increase in the clay content, which changes the structural framework of the material from a sand grain framework to a clay framework. The material approaches pure clay with clay contents above 30-50%, which is believed to decrease the erosion threshold (Grabowski et al. 2011). Mier and Garcia (2011) found results that coincide with this, with a lower average particle size resulting in a lower critical shear stress. However, while till is still considered a cohesive material, it has a wide range of particle sizes. Research should examine whether the large gravel particles embedded within the material alter the cohesive strength of the material in localized areas and cause irregularities in the surface where erosion is initiated.

2.5.1.2 Bulk Density

Most past research agrees that an increase in bulk density will cause a material to have a higher resistance to erosion (Grabowski et al. 2011; Krishnappan and Droppo 2006; Mier and Garcia 2011). Generally, bulk density increases with depth and therefore accounts for the variation in erodibility with depth in cohesive sediments. However this could also be due to the fact that with depth, the material is also subjected to less weathering and surface weakening (Grabowski et al. 2011; Houwing and van Rijn 1998; Krishnappan and Droppo 2006).

2.5.1.3 Water Content

Water content is inversely related to bulk density and thus an increase in water content generally causes material to be less resistant to erosion. A liquidity index greater than one indicates sediment that will behave in a viscous or visco-elastic manner, while a liquidity index less than one indicates sediment that will deform plastically. Generally, unconsolidated sediment, like freshly deposited estuarine muds, have a liquidity index greater than one and can become easily entrained. However, the till material used in this study is overconsolidated material that most likely has a low (less than one) liquidity index, and will therefore deform plastically. Govers and Loch (1993) found that a higher initial water content in cohesive sediment led to a higher resistance to erosion. This was thought to be because a disruption to the soil structure by microfissuration—the formation of microscopic cracks and fractures throughout the sample—might take place when an initially dry soil is rapidly wetted, and because initially wet soils allow a greater development of inter-aggregate bonds in the sediment which will decrease erodibility. This wetting-and-drying cycle can lead to weathering of the material which can greatly increase the erodibility. It is an important subject relevant to rising river stages, especially flood conditions, and is examined in more detail in the following section.

2.5.2 Weathering

Weathering, specifically the breaking down of the cohesive structure due to the formation of microfissures from wetting and drying, can greatly increase the erodibility of cohesive material (Lefebvre et al. 1986). Subaerial exposure can cause cracks and microfissures that quickly initiate erosion as a result of the weakening of the bank material due to weathering (Govers and Loch, 1993; Julian and Torres, 2006; Shugar et al. 2007). Gaskin et al. (2003) tested the effects of weathering on the Champlain Sea Clay from the banks of the St. Lawrence River by drying and rewetting the samples. The number of tensions cracks increased, and microfissures were formed, which resulted in a greatly reduced critical shear stress of the samples. It will be important to examine the effect of weathering, and specifically the wetting-and-drying cycle, on the erodibility of till material. Spring floods, heavy rainstorms, and increased surface runoff due to climate change and urbanization, will all cause rapid wetting to the till rivers in southern Ontario and its impact needs to be studied.

2.5.3 Vegetation

Research on the effect of vegetation on erodibility has shown mixed results. Vegetation is often present on the banks of rivers, but the vegetation cover can change over the seasons, resulting in the effect on the erosion process due to vegetation not being constant. Gaskin et al. (2003) studied the effects of a plant root structure on Champlain Sea Clay from the St. Lawrence River in a flume with a unidirectional current. They found the root structure to both help and hinder the erosion process. First, the cracks and fissures are easily formed around the roots in the clay structure. However, once blocks of clay have been delineated, the roots keep them in place so it takes longer for mass erosion to occur. The presence of vegetation over the clay banks subjects the clay to a lower shear stress because of the increased roughness. Overall, they found that vegetation increased the resistance to erosion of the clay banks. Coops et al. (1996) studied bank erosion and the interaction of waves on vegetation using a wave tank. They found the presence of vegetation greatly reduced erosion. The vegetation reduced the force of the waves hitting the banks, with the roughness from the plants slowing down the velocities. The study found that larger waves were capable of washing out some varieties of vegetation. They found that the waves washed sand into the vegetated banks which accumulated and increased the slopes, which led them to conclude that stable vegetated banks can have a steeper slope compared to unvegetated banks. Grabowski et al. (2011) also concluded that root networks work to stabilize the cohesive structure since a portion of the shear stress applied to the sediment will be transferred to the tensile strength in the roots. While vegetation is shown to influence the erosion of cohesive material, it is not examined in this study which primarily focuses on bed erosion.

2.6 Measuring Erosion

The critical shear stress, or erodibility, is often the parameter sought when quantifying erosion in research studies and when defining critical velocity of stress for design purposes in engineered river works, although the difficulty in quantifying it has been recognized. The critical shear stress is the stress required to initiate erosion, and is usually determined based on a visual assessment of the onset of erosion. Erodibility can also be defined in terms of a minimum erosion rate, which is the mass of sediment eroded per unit time once the threshold of erosion is exceeded (Grabowski et al. 2011; Mier and Garcia 2011). Adding to the difficulty in measuring erosion is the large variations in the composition and strength of clay and till at different sites, making studies difficult to compare.

Several methods have been employed to research the erosion process and determine the critical shear stress, which can be grouped into two general methods: hydraulic flumes and *in situ* jet-testers. The next two sections provide an in-depth analysis of these two methods and the results of past studies performed using them. When studying erosion, it is important to use a method which best represents the *in situ* conditions which the material is subjected to. Otherwise, the results may not be comparable to conditions in the field.

2.6.1 Flume Tests

Hydraulic flume tests are used to observe the erosion mechanisms and, in most cases, find the critical shear stress. They are performed by running a unidirectional flow over the cohesive material placed in the bed of the flume, with the top surface level with the bed and, in some cases, adjusted as the sample erodes. The erodibility is determined by incrementally increasing the water velocity in the flume until erosion is observed, at which point the critical velocity has been reached. Most flume tests are performed in the laboratory, presenting difficulties due to the need to preserve the sample during collection and transport. Researchers used to compensate for variability due to the disruption to the sample by remolding and reconsolidating the clay before performing tests. However, Lefebvre et al. (1986) did a comparative examination of critical shear stress values between remolded clay and natural, intact clay and discovered that the strength of the material greatly decreases after remolding, resulting in significantly lower critical shear stress values. The study noted the importance of maintaining the natural structuration of the material and preserving the natural bonds at the particle level. Therefore, the following studies reviewed in this paper are all those performed using intact samples.

Hydraulic flume tests have been performed in the laboratory by Kamphuis et al. (1990), Gaskin et al. (2003), and Mier and Garcia (2011), and in the field by Debnath et al. (2007). All three laboratory studies found mass erosion to be the predominant form of erosion, and that for a particular velocity the rate of erosion was rapid at first, decreasing with time. Mass erosion was observed as blocks of clay breaking off from areas with discontinuities, which included protruding gravel particles for the till. Gaskin et al. (2003) noted a similar process for Champlain Sea clay, with already-present cracks and fissures enlarging, eventually breaking off into blocks of clay, and areas without cracks or fissures becoming more polished. The critical shear stress values obtained from these studies have been summarized in Table 1. While the flume tests provided a good means to observe the mechanisms of erosion, there is unavoidable damage to the sample during cutting and transport that can alter the critical shear stress values. The use of an *in situ* flume by Debnath et al. (2007) tried to mitigate this problem.

Table 1: Critical shear stress values of previous studies

Study	Apparatus	Material	Average Critical Shear Stress (Pa)
Kamphuis et al. (1990)	Flume	Silty Clay	2.56-4.1
		Glaciolacustrine Silty Clay	0.88
		Silty Till	0.65
Gaskin et al. (2003)	Flume	Champlain Sea Clay	6 - 20
Mier and Garcia (2011)	Flume	Till	4.2
Shugar et al. (2007)	*in situ* Jet-Tester	Fletcher's Creek Halton Till	2.28
Khan and Kostaschuck (2011)	*in* situ Jet-Tester	Fletcher's Creek Till	5.43
		Highland Creek Till	22.7

Debnath et al. (2007) used an *in situ* flume tester to study the erodibility of cohesive stream banks in an effort to diminish any change in material properties during transport from the field to the laboratory and to more accurately represent the flow conditions. Similar to the other studies, the rate of erosion was found to be most rapid at first and diminishing over time. Erosion was found to be predominately bed-load transport with only negligible resuspension processes. While effort was used in this study to minimize disturbance to the sample, the flume test still required the material to be cut out of the river, albeit never removed from the river entirely, and therefore subjected the samples to unavoidable damage. Unfortunately, the critical shear stress values were not obtained from this study and so those results cannot be compared to the other flume tests.

The ability to observe the mechanisms of erosion of the cohesive material make hydraulic flumes a popular choice, but damage to the sample during transport can alter critical shear stress values. It has been determined that erosion initiation predominantly occurs at irregularities or discontinuities, and the addition of these weak areas due to the transport process can have a large influence on when and where erosion will initiate. In this regard, using a hydraulic flume to study erosion may be a good choice for qualitative observations of the mechanisms of erosion, but there is a chance that the quantitative values of the critical shear stress are inaccurate.

2.6.2 *In situ* Jet-Testers

In situ jet-testers can be used vertically or horizontally, on the bed or the banks of a river, in order to obtain a critical shear stress of the material. The jet-testers subject the material to a jet of water directed at a small point on the surface, and the depth of scour is measured at set time intervals until the depth no longer increases. Two assumptions are made: 1) the final depth represents the scour depth at which the stress at the boundary is no longer enough to cause additional downward stress (i.e., critical stress), and 2) the rate of change in depth of scour before the depth no longer increases is due to the maximum stress at the boundary and the erodibility coefficient (Hanson and Cook 1997; Khan 2011). Using the measurements from the field, and an analytical spreadsheet developed by Hanson and Cook (1997), the critical shear stress is estimated based on the velocity of the jet, the depth of the scour, and friction and drag coefficients determined by experimental work.

In situ jet-testers have been used by Shugar et al. (2007) and Khan and Kastaschuck (2011) to test the erodibility of till from southern Ontario. Both studies tested Halton till from Fletcher's Creek in Lake Ontario, while Khan and Kastaschuk (2011) also tested Sunnybrook till from Highland Creek in Lake Ontario. Several locations were tested at each site to determine the spatial variability of critical shear stress. For both studies, the critical shear stress of the Halton till varied by up to five orders of magnitude at different locations; however, there were no apparent spatial or temporal patterns. Khan and Kastaschuck (2011) also found the critical shear stress for Sunnybrook till varied by three orders of magnitude. The critical shear stress results of each study are summarized in Table 1. In terms of the mechanism of erosion, field observations of the two sites showed that the Sunnybrook till experiences mass erosion, with the sediment eroding as aggregates, or along micro-fissures and cracks, and that the Halton till experiences surface erosion, eroding as individual particles and small flocs.

In situ testing is advantageous because it ensures the material will not be damaged as it is not extracted or transported, however the limitations of the jet tester far outweigh the advantages and might explain the wide range of results. It is difficult to use an apparatus *in situ* that can test the critical shear stress while also closely mimicking unidirectional flow conditions and tangential stress and isolating for specific parameters. The basic principle of the jet tester method is in question since it drills a hole in the surface and no longer induces a tangential stress to the surface of the material. Even though mass erosion was observed in the field, the jet tester does not allow the material to undergo mass erosion because it is a structural process larger than the scale of the testing device. Since the device is only capable of testing localized erosion, the large variation in the surface shear strength for the tills could be due to small differences or irregularities in the surface topography. Additionally, after each measurement, the operator must remove large particles, or gravel pieces, that are within the test hole (Shugar et al. 2007). The abrasion due to these gravel particles, and any sand particles trapped in the scour hole, during the test could greatly affect the results (Kamphuis et al. 1990). The critical shear stress values obtained from studies using jet-testers is highly questionable because the test does not represent reality in terms of stresses the material is subjected to by the river flow.

3.0 Methods

3.1 Project Description

To address the research objectives of determining the critical shear stress of till and increasing the understanding of the role of the alluvial cover, flume studies were performed on several samples collected from the river bed of Medway Creek, a tributary of the Thames River in London, Ontario (Figure 2).

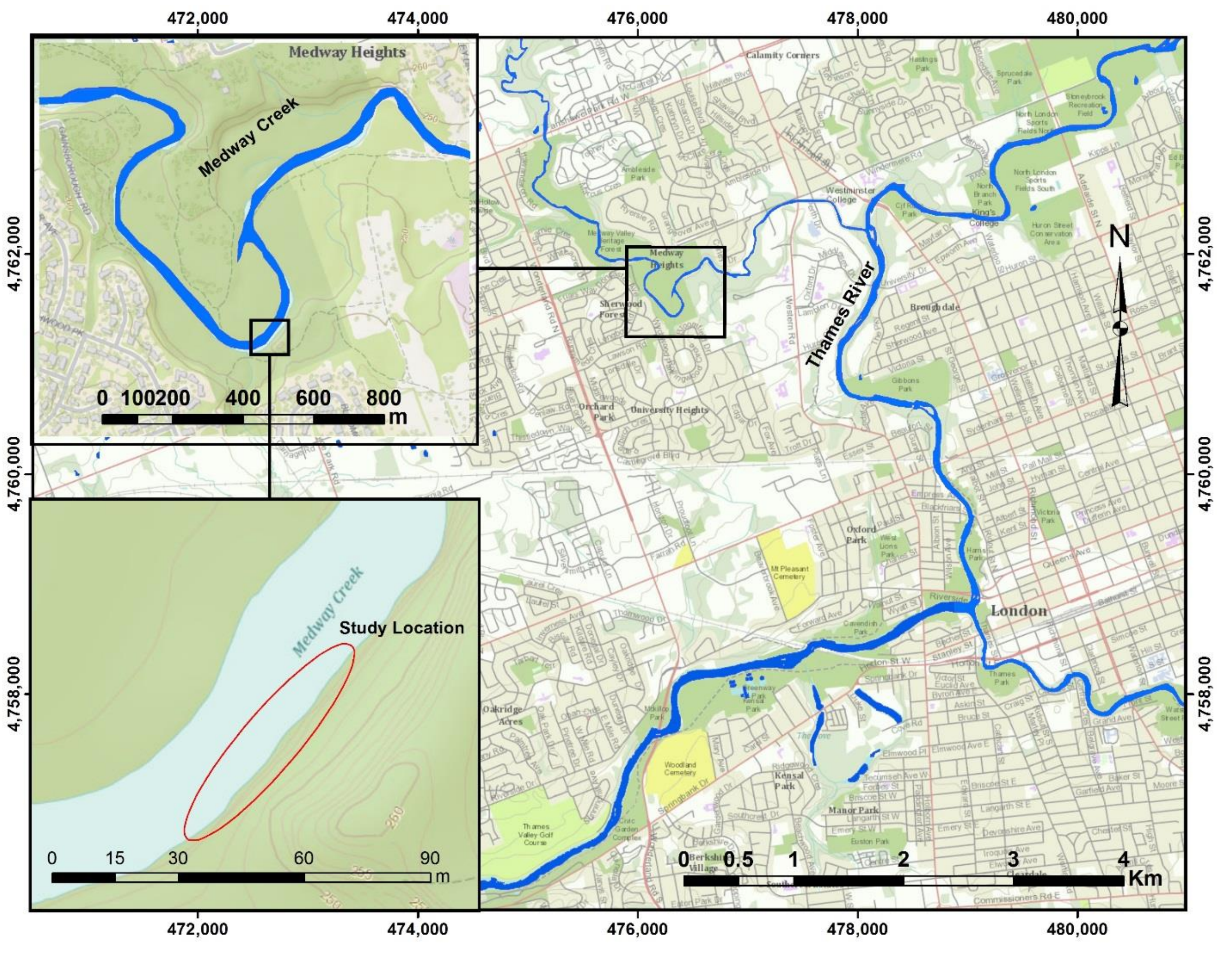

Figure 2: Location of study reach, Medway Creek, London, ON.
Grid is NAD1983 UTM zone 19N (m). (ESRI World Topo Basemap)

Performing the tests in a laboratory flume was chosen because a flume best allows for the observation of the mechanisms of erosion since the entire process of erosion is able to proceed. Flume tests also subject the material to a shear stress environment similar to that of the river and allows for the determination of the critical shear stress in a controlled environment. However, samples undergo some unavoidable disturbance and damage due to the extraction, transport, and storage processes involved with laboratory testing. Nevertheless, this testing method was still chosen because it best represents realistic river conditions and allows for all parameters of interest (wetting/drying and presence of alluvial cover) to be tested.

The study location was chosen due to the underlying till, past research in the area, and its proximity to the University of Western Ontario campus. Till, deposited during the Wisconsin glaciation, forms the upper layer of geologic materials of the Thames River and its tributaries (Thames 1989). Figure 3 is a physiographic map that shows the extent of till in the southern Ontario region. Foster (1998) and Hrytsak (2012) have previously performed studies on the morphology of the alluvial cover on Medway Creek, albeit not specifically related to till erosion. This study plans to extend the research by determining the critical shear stress of the till and, with regards to the semi-alluvial aspect of the area, focus on how the presence of alluvial material impacts the erosion of the underlying till. The proximity to the University campus and ease of public access helped the collection process, and was considered in the site selection along with the fact that some previous research had been conducted at the site related to channel geometry.

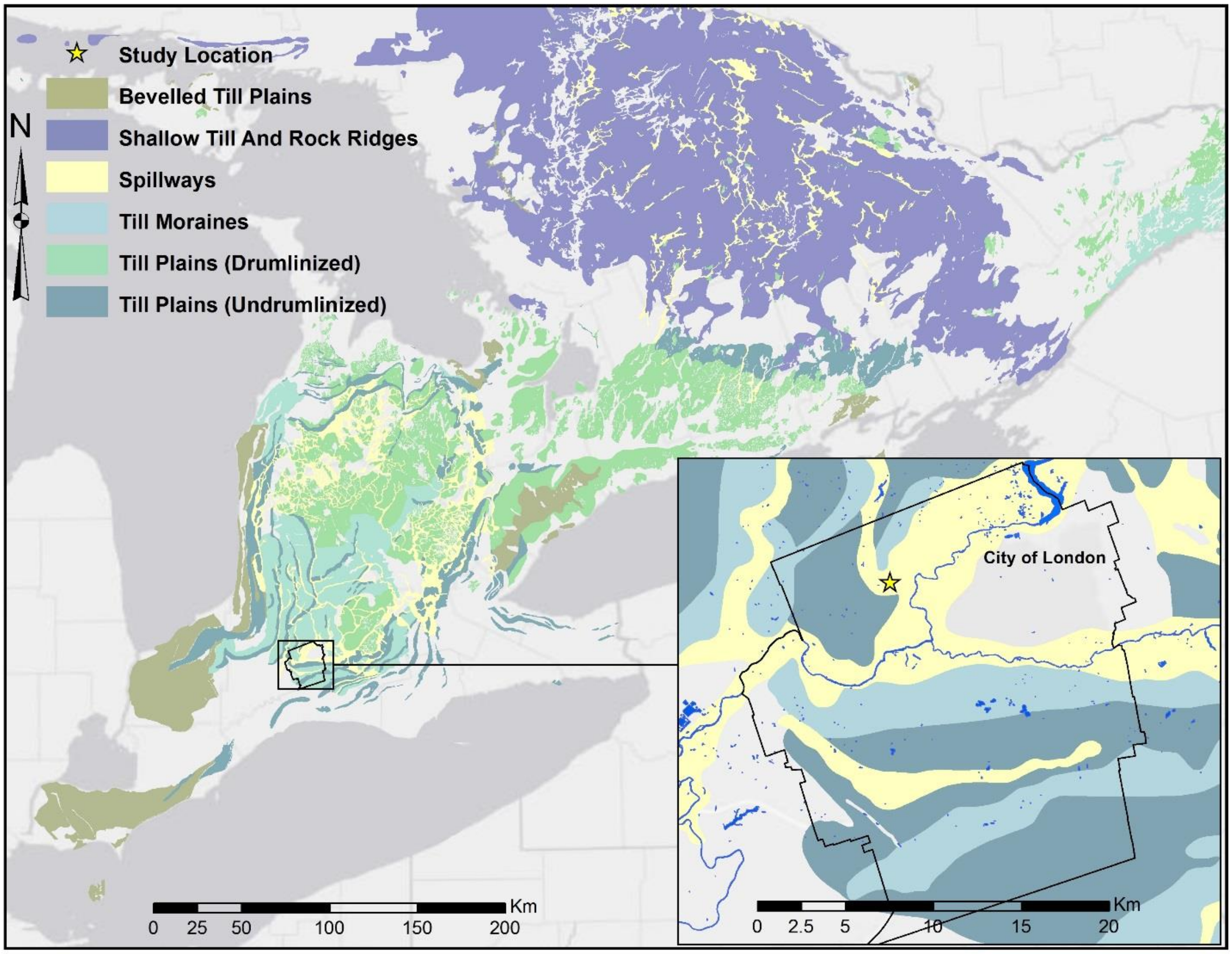

Figure 3: Physiography of southern Ontario (Chapman and Putnam 1984)

The flume testing scheme was developed to address the research questions in the most feasible manner. A total of six samples were tested: two samples at their natural moisture content to obtain the critical shear stress, two samples that were air-dried before testing to determine the erosion impacts of wetting and drying, and two samples at their natural moisture content with gravel present in the flow to understand how the gravel particles interact with the sample and what their effect on erosion is. The sample size was small because of the difficulties involved in sample collection. Due to this, three tests were chosen to investigate the most important factors influencing erosion. Unfortunately there were not enough repetitions of the same test to assess reproducibility of the results. The sample collection process and details of the hydraulic flume tests are outlined in sections 3.2 and 3.3.

3.2 Sample Collection

Samples were collected from Medway Creek to be used in hydraulic flume tests in the McGill University hydraulics laboratory. They were taken from the right bank in the study area outlined in Figure 2, and seen in Figure 4. Samples were collected by hand in the form of large blocks of till that had previously been dislodged from the river bed and were resting on the bed, but still submerged in the river. The river bed material at Medway Creek (Figure 4) is difficult to penetrate with hand tools such as shovels, and the river is an "Environmentally Significant Area" which does not allow any excavating equipment to be used. However, because the samples were collected by hand, they were not subjected to additional stresses from shovels or other extraction equipment and therefore all present damage is assumed due to natural weakness. Care was taken to prevent damage to the samples during extraction and transport.

Figure 4: Downstream view of study site on day 1

The samples were extracted from the river over a period of three days. They were wrapped in multiple layers of plastic to preserve their moisture content and stored in bins surrounded by bubble wrap to minimize damage during transport. The samples were transported back to Montreal and subsequently stored in a humid room (Geotechnical Laboratory, Civil Engineering, McGill University) until used to help prevent unwanted drying.

A sample of the gravel cover was collected from the edge of the river (Figure 5) to be used in the flume studies. The median particle size for the 78 collected gravel particles, D_{50}, was calculated to be 23 mm (see section 5.2). Bed material samples collected in the reach by Hrytsak (2012), using standard sampling procedures for fluvial gravel, had a D_{50} of 45 mm. The gravel collected for the flume experiments represents the finer fractions of this river bed material because the larger particle sizes were impractical for the flume and till sample dimensions.

Figure 5: Gravel sample collection site

3.3 Flume Studies

A recirculating hydraulic flume, which is a rectangular channel with a unidirectional current, was used to test the samples. The hydraulic flume used for testing, shown schematically in Figure 6 and Figure 7, is a 4 m long, 40 cm wide channel, with a depth of 15 cm.

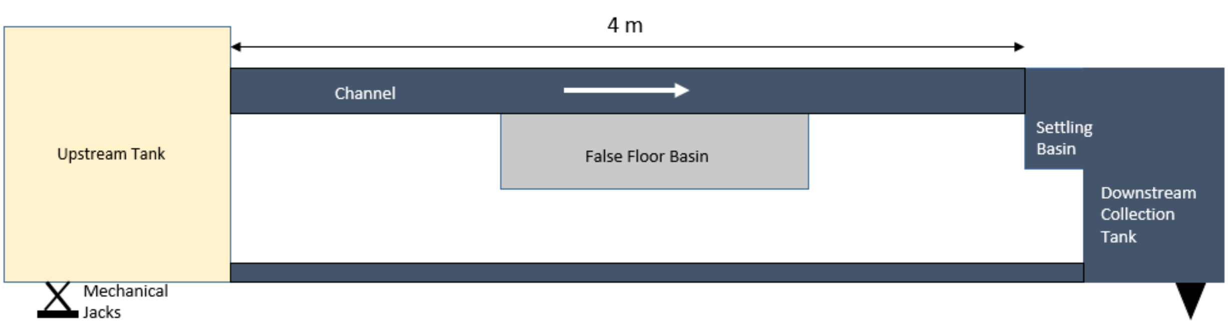

Figure 6: Hydraulic flume, elevation view

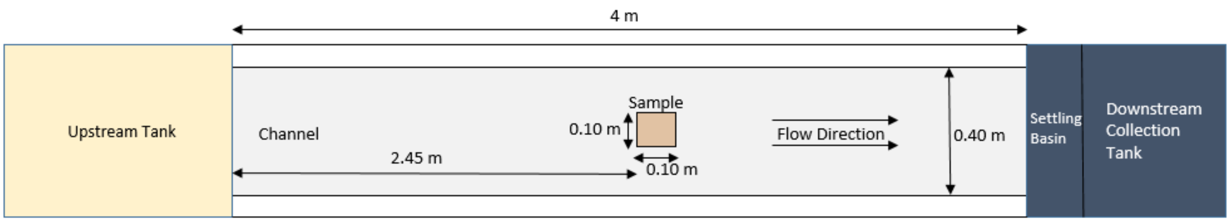

Figure 7: Hydraulic flume, plan view

The flow was recirculated from the downstream collection tank back to the upstream tank using a pump, which has a maximum flow capacity of approximately 13.8 L/s. The discharge was measured with a Midwest Instruments and Controls "In-Line Digital Flow Meter" (micro propeller flow meter) placed between the pump and the upstream tank. In order to adjust the flow and change the applied shear stress on the sample in the flume, two valves were installed immediately downstream of the pump which enabled control of the flow and also careful stopping and starting of the pump itself. The pump was stopped overnight by closing one of the valves to slow down the flow in order to prevent overflow from the channel due to an abrupt stop of the pump. The other valve was untouched in order to preserve the flow rate for when the pump was started again the next day. The slope of the flume was adjusted to increase or decrease the applied shear stress on the sample; this was done using mechanical jacks at the upstream end of the flume and measured using a surveying level. Assuming uniform flow in the channel, the bed shear stress was calculated, using the equation:

$$\tau = \gamma_w S R$$

where γ_w was assumed to be 9810 N/m^3, S was the measured slope of the flume, and R was the hydraulic radius, calculated using the width of the channel and the depth of water measured with a point gauge with a resolution of 0.1 mm (Figure 8). The depth of water was measured in the center at the upstream edge of the sample and the point gauge was calibrated to zero at this point.

The point gauge was recalibrated to the flume floor several times throughout the experiment and for each sample.

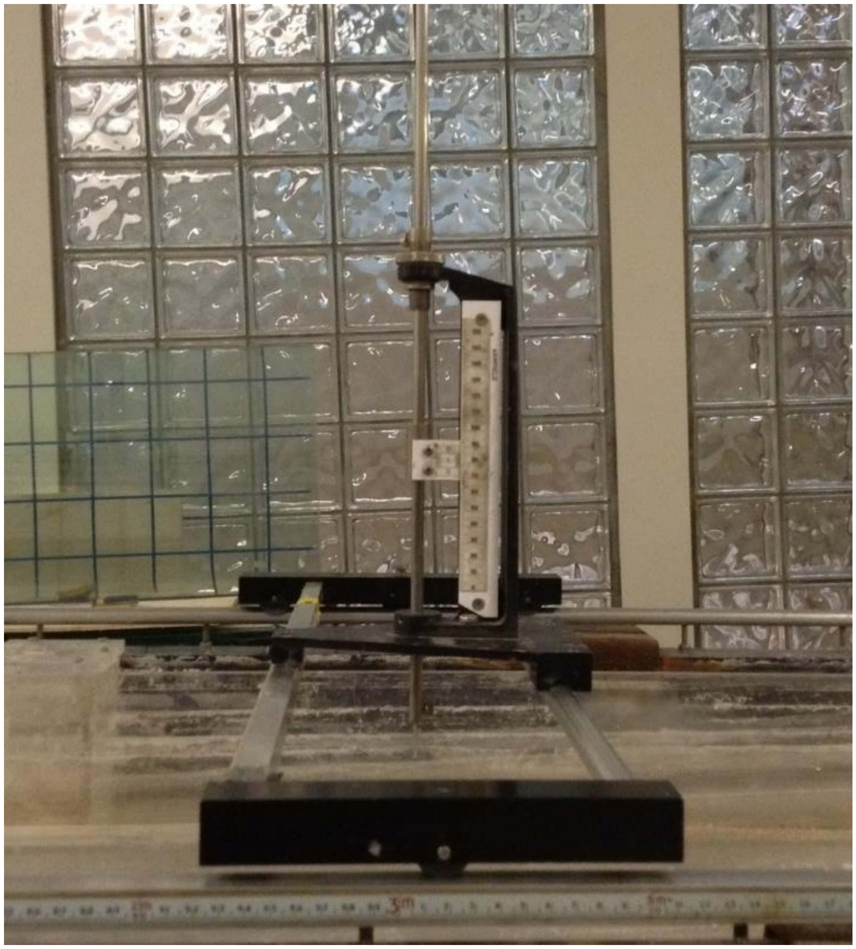

Figure 8: Measuring point gauge

Each sample was placed in the flume such that the top surface of the sample was flush with the channel floor to ensure no forces were exerted on the sample besides the bottom shear stress of the flow. This was achieved by placing the sample on a height-adjustable platform beneath the flume's plexiglass false floor in a 10 cm x 10 cm hole, located at a distance of 2.5 m from the upstream end of the channel (Figure 9). The platform was adjusted throughout the tests to raise the sample while it eroded so the surface of the sample was level with the flume floor at all times. For some samples, this only needed to occur a few times throughout the entire test, while others required adjustment approximately every 5 minutes.

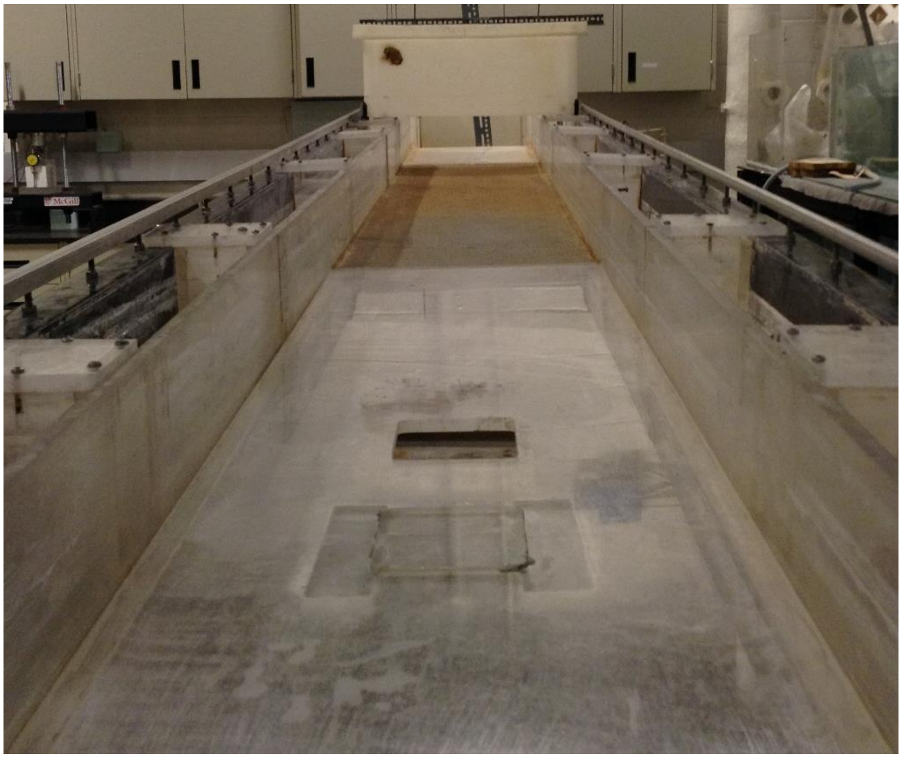

Figure 9: Hydraulic flume channel showing sample location

The samples were prepared for the flume by removing them from the humid room, where they were stored, and then submerging them in water in a bin for at least 12 hours (overnight) before cutting them to their sample size. This measure was implemented after it was discovered that submergence can cause the till material to split apart. The splitting indicates that there was possibly some drying of the samples, which is an adverse effect of storing the samples. Submerging the samples before cutting allowed them to return to river conditions in terms of their moisture content before testing began. After submergence, the samples were cut into cubes of 10 cm x 10 cm with heights varying from 7-10 cm, depending on the uncut shape of the block. A diamond masonry saw was used for cutting as it was capable of cutting through the large gravel particles in the sample without causing any apparent damage. After cutting, the samples were taken to the hydraulic flume.

The hydraulic flume was used to find the critical shear stress and observe the mechanisms of erosion. A general overview of the flume test is now provided, followed by specific details regarding the testing of each sample. Each sample was placed in the flume and subjected to a unidirectional current of supercritical flow in order to apply a uniform shear stress to the surface of the material. There were no waves present in the flow for the first four samples, which allowed for precise flow depth measurements. The final two samples had gravel present in the flume which caused turbulence and made precise flow depth measurements more difficult. Testing began with a low flow rate, and hence, low applied shear stress. The shear stress on the sample was increased in small steps by incrementally increasing flow rates. Because the valve could not precisely regulate the flow, the flow rate and shear stress increments were not exactly the same in all tests, but effort was used to ensure the shear stress did not increase more than 1 Pa between increments, with the increments generally ranging from 0.5-1 Pa, and then 0.1-0.3 Pa in higher shear stress ranges. At each increment, the erosional effects, if any, were observed. The critical shear stress was taken as the shear stress at which erosion was first visible. If no erosion was apparent at a given shear stress (flow rate) after 15 minutes, or if any erosion ceased during the test, the shear stress (flow rate) was increased. 15 minutes was used because past studies have shown that erosion will occur rapidly at first and decrease over time, thus, if any erosion were to occur at a given shear stress, it should happen early in the time period (Kamphuis et al. (1990); Gaskin et al. (2003); and Mier and Garcia (2011)). Once erosion began, the shear stress was held constant until erosion was no longer visibly apparent, which was usually on the order of hours, before it was again increased. Testing stopped after the sample had either eroded completely or had been subjected to the highest shear stress possible, approximately 8.9 Pa, and all erosion had ceased. Observations and pictures were taken at each applied shear stress in order to determine the critical shear stress and the erosion mechanism.

To address the research question about the magnitude of the critical shear stress of the material, Samples 1 and 2 were tested with their natural moisture content under clear water flow. This scenario best represents the bed of a river, since this area is rarely subjected to drying, where the till is exposed (no alluvial covering). The procedures for these two tests did not vary from the description given above.

In order to determine how weathering, and specifically a wetting-and-drying cycle, impacts the erodibility of till, Samples 3 and 4 were tested under air-dried conditions. This scenario is representative of the banks of a river where the till can dry when the river stage is very low between high flow events. After the samples were cut to their sample size, they were placed on the platform in the flume and allowed to dry for approximately 48 hours to ensure they were dry throughout. At this point, both samples appeared to be visibly dry and ready for testing. It would have been possible to calculate the average moisture loss by weighing the samples after they were cut and then again after the 48 hours, but unfortunately, this was not done. The samples were then lowered into the flume and testing began immediately. This represents banks that are subjected to either flood conditions or increased surface runoff, in which case the banks are quickly submerged and exposed to shear stresses. The flume testing then proceeded in a similar manner to Samples 1 and 2.

Sample 5 and 6 were tested with the collected gravel sample present in the flow in order to elucidate the effect on erosion of large particle impact and/or covering of the sample. These samples were cut to size and put into the flume with their natural moisture content, similar to

Samples 1 and 2. The collected gravel sample was placed in the flume upstream of the till sample, and a collection cage was used at the downstream end of the flume to collect the gravel particles. Flume testing then proceeded in a similar manner to all the other samples, except that once all of the gravel particles arrived at the downstream end of the flume, they were collected and manually brought back upstream to be recirculated. This allowed for a continuous supply of gravel during testing, however, there were small periods of time when no gravel was in the flume while it was being manually transported from the downstream end to the upstream end.

3.4 Measurement Uncertainties

There were several quantitative uncertainties within the testing procedure that are evaluated to determine the quantitative uncertainty in the observed shear stress value. The uncertainty in the critical shear stress was a function of the uncertainty in the measured slope and hydraulic radius and in the visual determination of the onset of erosion. Measurement uncertainties due to the resolution of the point gauge, measuring rod used in levelling the flume, and tape measure used in measuring the length are easily quantified. The uncertainty that resulted from determining the critical shear stress that corresponded to the onset of erosion was assumed to be one-half the applied shear stress increment during which onset of erosion occurred. The overall uncertainty of each measurement is listed in the results and in Appendix VI.

3.5 Material properties

Several tests of material properties were performed on the samples to get a better overall understanding of the material. These included:

- moisture content
- bulk density

- specific gravity
- particle-size distributions of till and gravel samples

The moisture content was calculated immediately after testing the sample to obtain a representative moisture content during testing. It was not determined beforehand so as not to disturb the intact sample. However, in the cases of Samples 3 and 4, which were air-dried before testing, testing the moisture content immediately afterwards is not representative of the moisture content of the sample during testing, and additional assumptions had to be made. The tests for bulk density, specific gravity, and the particle size distribution were performed on the parts of the sample that were trimmed while the sample was being cut. The particle-size distribution for the till was only obtained for Samples 1, 2, and 4, because Samples 3 and 5 did not have enough extra material after being trimmed to perform the test, and the results of the three samples tested were similar enough that is was assumed they accurately portrayed the particle size distribution of the material in the sampled area. The particle-size distribution was also measured for the collected gravel sample.

4.0 Study Site and Field Work Observations

The nature of the till in the bed and banks of Medway Creek was examined in the field at the time of sample collection. In-situ observations of the internal structure (joints and bedding), the response of the till under a wetting-and-drying cycle, and the presence of alluvial material in the area were made. Figure 10 is an image of the till bed under water.

Figure 10: Till bed

The till was very dense and hard; it could not be penetrated with a shovel by hand and the specific gravity of the samples was later calculated to be an average of 2.36. Observations indicated that the till banks have a natural planes of weakness and defined fractures. In some cases, these fractures were similarly oriented and actual fracture planes were observed (Figure 11). The apparent structure of the material, and the abundance of chunks of till on the bed where erosion had taken place, was evidence of mass erosion (Figure 12). Mass erosion was also observed as block separation under the water (Figure 13). Larger gravel and cobbles could be seen embedded in the till.

Figure 11: Fractures in till banks

Figure 12: Chunks of till eroded at Medway Creek bank

Figure 13: Block separation under water

The wetting-and-drying cycle appears to weather the material and increase erosion by causing tension cracks during drying and then a break-down of the cohesive structure when re-wetted. This phenomenon was observed during a thunderstorm with intense rains that took place between Day 1 and Day 2 of sample collection (September 10th and 11th, 2014). On Day 1, the exposed till banks of Medway Creek were dry, with evident tension cracks in many locations. Figure 14 shows the base of a dry river bank where tension cracks are apparent in the till (right corner of the image). The image also portrays the rough and jutted surface of the till itself due to the mass erosion. Figure 15 is a close-up image of a dried section of the bank showing more cracks.

Figure 14: Dry till banks at Medway Creek

Figure 15: Tension cracks in banks at Medway Creek

On Day 2, after the intense rainstorm, areas in the river bank that had previously been dry, cracked, and rough on the surface, had become wet and slumped over, having lost material and the surface now being smoother. Figure 16 shows the bank on Day 2, after the rainstorm. The vertical nature of the banks indicate the cohesive nature of the material (the bulk strength) and also the undercutting pattern of erosion, in which the material is eroded at the water level and then the overlying bank falls in. The height the water level reached on the bank was apparent and can be seen in the circled area of the image. The till below the water line, or the material that had been submerged, had a smooth surface, indicative of having lost material and the eroded material slumping down towards the river.

Figure 16: Slumped till bank at Medway Creek

There was a strong presence of alluvial material in the form of large gravel particles embedded within the till itself, intermittently covering the bed, and at the foot of the banks of the river. Gravel embedded in the till and partially exposed can be seen in Figure 11. Figure 17 shows a small lateral bar of gravel on the far bank of the river at the collection site. A discontinuous alluvial cover could be seen on the river bed. Unfortunately, no pictures were taken of the alluvial cover on the bed on Day 1, and the river was too turbid on the following days to see it. However, Hrytsak (2012) studied this particular reach and noted that the alluvial cover varied within the reach and had an overall thickness of 30 cm or less. Figure 18 shows exposed till underneath the alluvial covering and gives a good sense of the extent of alluvial covering in some areas of the river which is estimated to be between 50-70% by area (Hrytsak 2012). Hrytsak (2012) also determined a particle size distribution of the alluvial cover, and calculated an average grain size of 45 mm (Figure 19).

Figure 17: Gravel along bank at Medway Creek

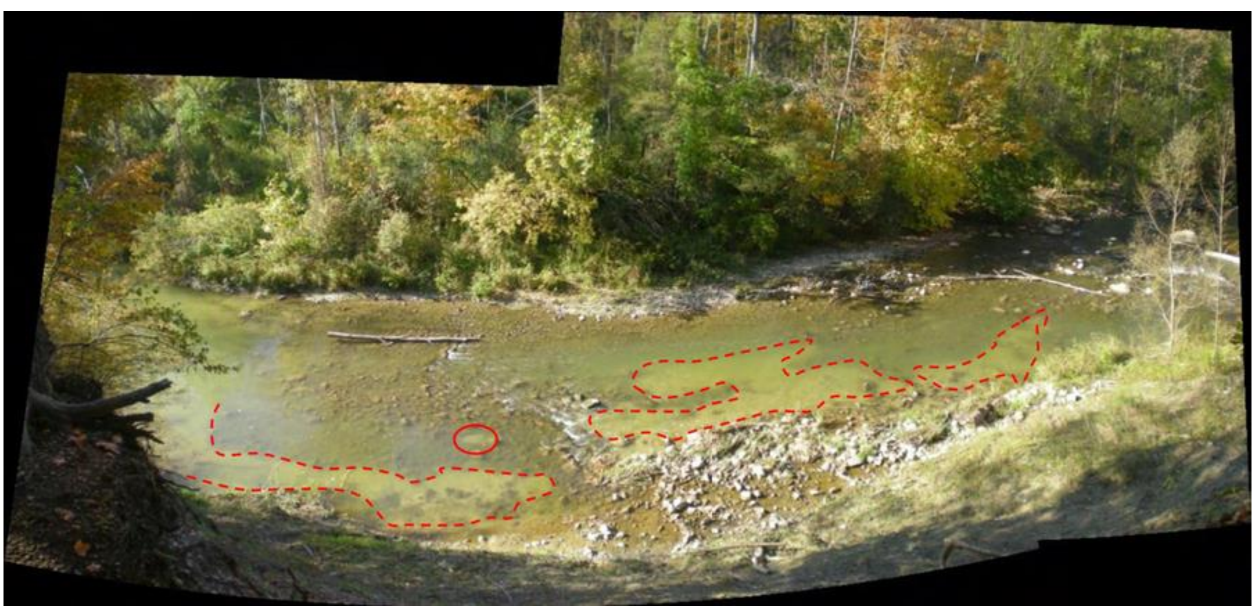

Figure 18: Intermittent alluvial cover with till exposures outlined in red (Hrytsak 2012)

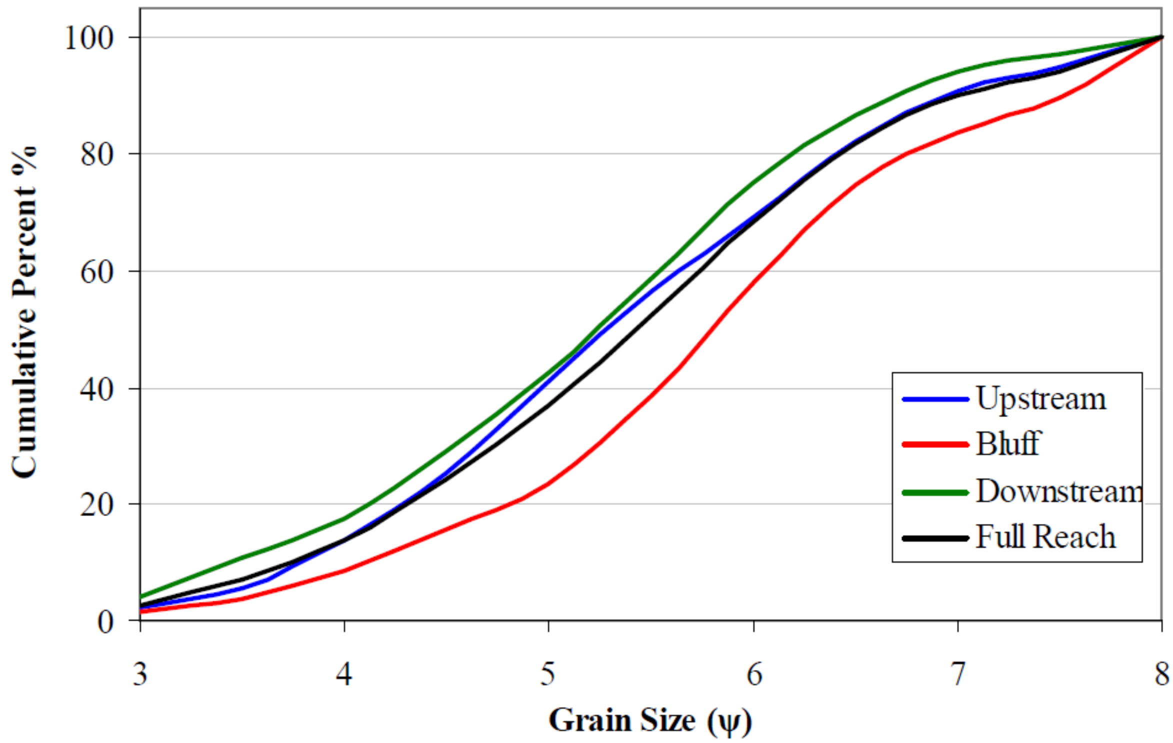

Figure 19: Cumulative grain size by area for Medway Creek (Hrytsak 2012)
Note: horizontal axis is an inverse psi scale, where 3 = 8 mm, 4 = 16 mm, 5 = 32 mm, etc.

Visiting the field site confirmed the expected character and behavior of the material. The till undergoes mass erosion in the field in the form of blocks of material eroding from the bank. The wetting-and-drying cycle had a noticeable effect on the erosion of the till material and it is important to determine its impact on the critical shear stress. There is a significant alluvial deposition, especially of gravel-sized particles, that might be a significant factor in erosion of the till.

5.0 Test Results

5.1 Observations and comments about the nature of the till

The samples of till used throughout this study proved to be very brittle and there was a presence of wormholes throughout some of the samples. The till is dense with an average specific gravity of 2.36, and its brittleness was evident as it was easily cracked and split apart with handling. The material would undergo "clean breaks" across the sample, which appeared to be already-present planes of weakness. To avoid cracking, the material was handled extremely carefully. Nevertheless, the brittleness of the material resulted in many samples needing to be recut due to cracks formed before testing. In addition to the brittleness, blood worms and worm holes were found intermittently within the sample. The distribution within the volume of the sample of the worms and wormholes was irregular. The samples used in testing were free, or mostly free, of the wormholes, except for Sample 6 in which worm holes were exposed once the sample had eroded (see section 5.3.7).

5.2 Sample Properties

The results of the sample properties tests are shown in Table 2. It is important to note that the moisture content tests were performed immediately after the flume tests. For the air-dried samples, 3 and 4, the initial moisture content is unknown but assumed to be low due to the air-drying process. However, due to the nature of erosion in those particular cases, the moisture content immediately after testing for these two samples is significantly higher relative to the other samples. Results of the particle size distribution tests for the till samples 1, 2, and 4, are shown in Figure 20. According to the particle size distribution, the till samples are composed of 8% gravel, 20% sand, 29% silt, and 43% clay, with a D_{50} value of 0.0065 mm, which corresponds to "very fine silt" (Wentworth 1922). The calculated particle size distribution for the collected gravel sample is shown in Figure 21, with a D_{50} value of 23 mm, which corresponds to coarse gravel (Wentworth 1922).

Table 2: Sample properties

	Moisture Content (%)	Bulk Density (kN/m^3)	Specific Gravity
Sample 1	10.9	26.1	2.31
Sample 2	10.8	25.1	2.33
Sample 3	24.3	26.1	2.47
Sample 4	23.2	24.5	2.30
Sample 5	11.1	25.0	2.33
Sample 6	11.8	25.6	2.44

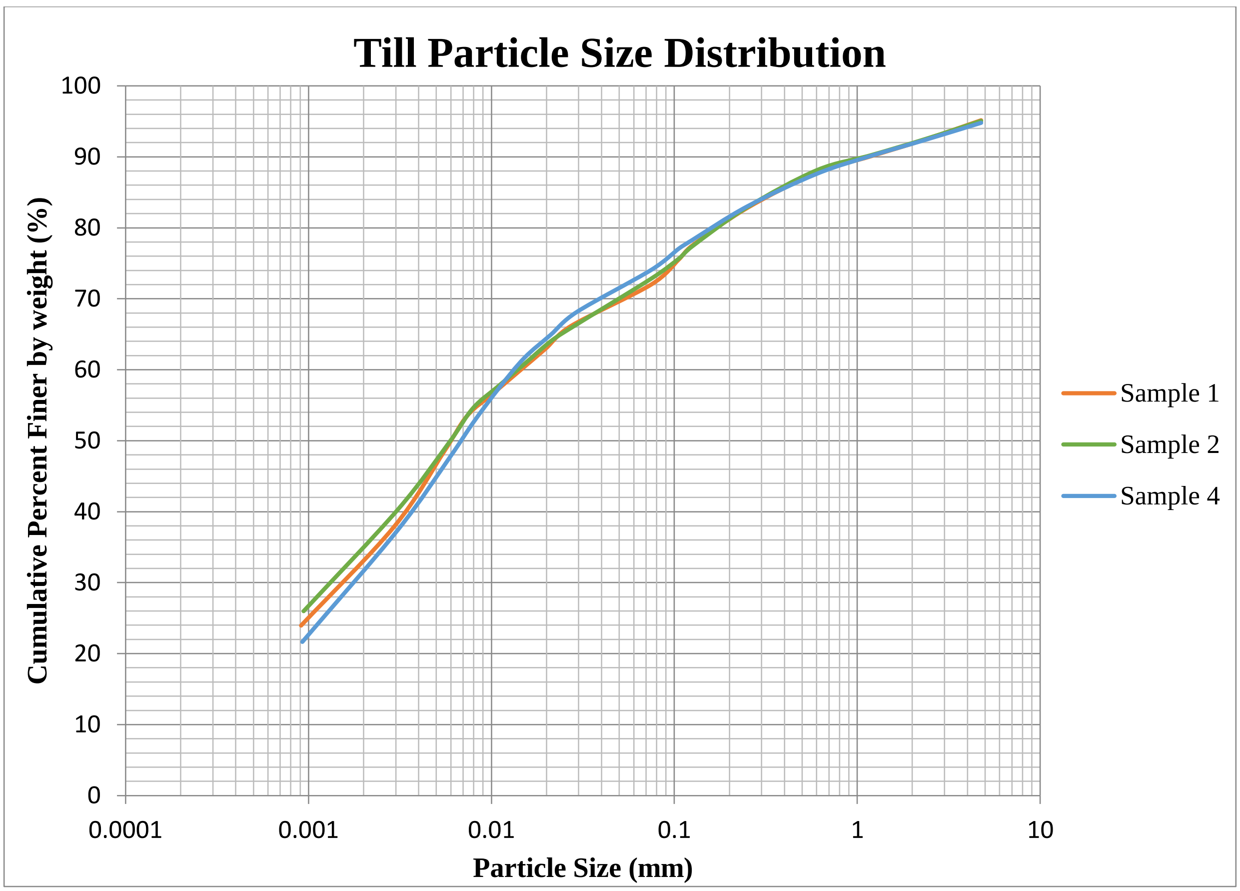

Figure 20: Till particle size distribution

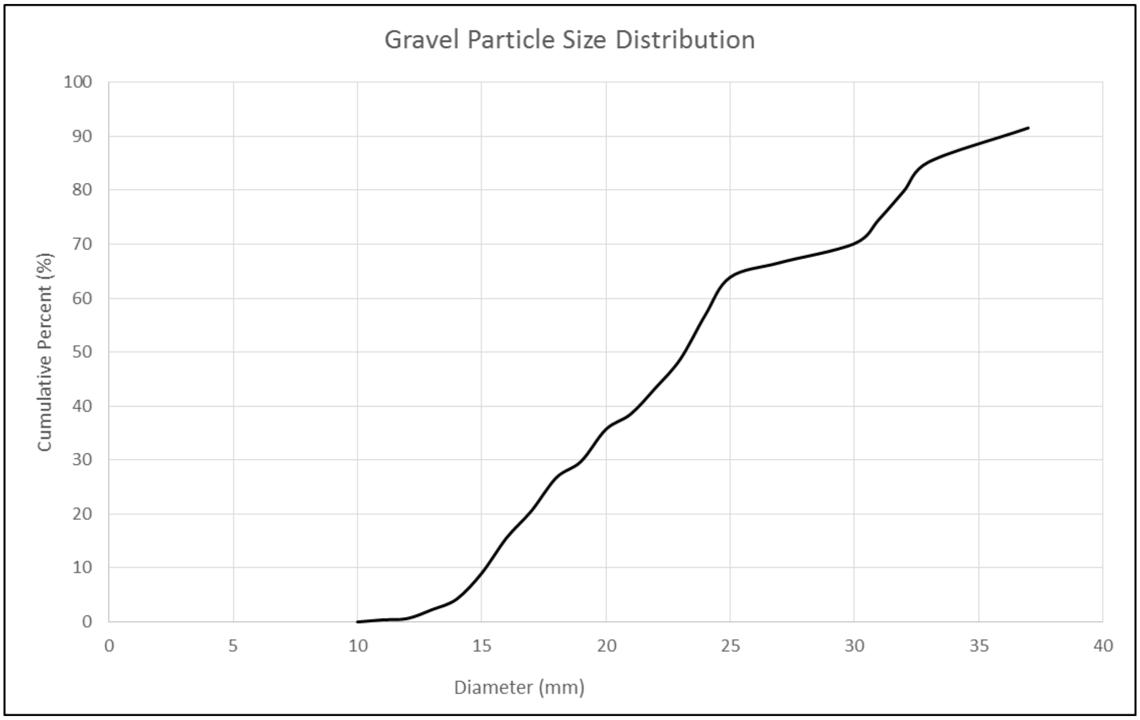

Figure 21: Gravel particle size distribution

5.3 Flume Studies

A summary of the critical shear stresses observed in the flume studies is provided followed by a detailed description of each test.

5.3.1 Summary of flume results

The critical shear stress values for the six samples obtained from the hydraulic flume studies are summarized in Table 3 below. A graph of the applied shear stress values over time has also been created indicating the critical shear stress for each sample Figure 22.

Table 3: Summarized results of flume studies

Sample	Test Description	Critical Shear Stress (Pa)
1	Normal moisture content	7.9 +/- 1.0
2	Normal moisture content	8.3 +/- 0.9
3	Air dried	1.2 +/- 0.8
4	Air dried	0.9 +/- 0.6
5	Normal moisture content, gravel abrasion	6.8 +/- 0.7
6	Normal moisture content, gravel abrasion	4.3 – 6.1

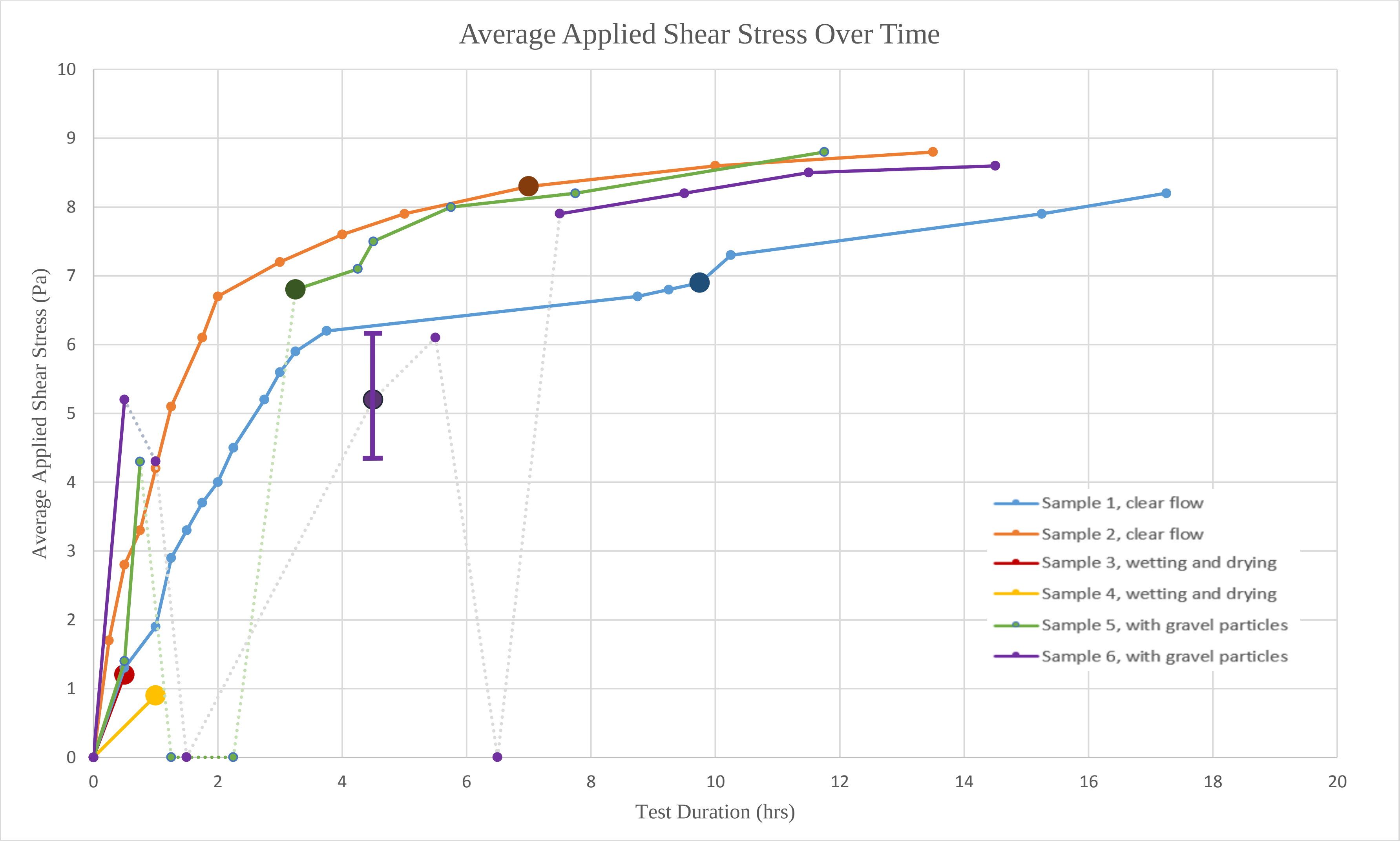

Figure 22: Average applied shear stress over time for each sample, with critical shear stress in bold.
Note[1]: Only the range within which the critical shear stress for Sample 6 lies could be observed (4.3 – 6.1 Pa), as shown in the figure.
Note[2]: The dotted lines for Samples 5 and 6 show when the gravel covered the sample, and thus, the average shear stress was unknown, but assumed to be close to 0 Pa.

5.3.2 Sample 1

Sample 1 was tested to find the critical shear stress of till at its natural moisture content under clear flow conditions. The sample eroded through mass erosion, by fracturing and delineating small chunks of till which eventually dislodged from the sample. The first sign of weakening of the till was a crack that developed down the middle of the sample, which occurred at an applied shear stress of 6.7 Pa, appearing to split the entire sample in half. With a further increase in the applied shear stress to 7.9 Pa, a chunk of till adjacent to the crack became dislodged and eroded, and this point was assumed to be the critical shear stress of the sample. A further increase in the critical shear stress did not yield more mass erosion, however, embedded gravel pieces within the surface of the sample were slowly revealed as the clay matrix of the till slightly eroded from the surface. Sample 1 did not have a flat surface at the edges of the sample due to the size of the sample before cutting and the fragile nature of the till. This was taken into consideration during testing, and any breakage or erosion that occurred in these areas was discounted. Table 4 summarizes the testing conditions of Sample 1 as well as relevant observations. Figure 23 shows the various stages of erosion the sample underwent, and Figure 24 shows the sample before and after erosion.

Table 4: Sample 1 flume test and observations

Duration (hrs)	Discharge (L/s)	Slope	Depth of Water (cm)	Shear Stress (Pa)	Observations
0.5	1.5	0.031	0.42	1.3	No apparent erosion
0.5	2.5	0.031	0.65	1.9	No apparent erosion
0.25	4.2	0.031	1.00	2.9	No apparent erosion
0.25	5.2	0.031	1.15	3.3	No apparent erosion
0.25	6.1	0.031	1.30	3.7	No apparent erosion
0.25	6.9	0.031	1.40	4.0	No apparent erosion
0.25	8.2	0.031	1.61	4.5	No apparent erosion
0.5	9.9	0.031	1.86	5.2	No apparent erosion
0.25	10.9	0.031	2.01	5.6	No apparent erosion
0.25	11.7	0.031	2.16	5.9	No apparent erosion
0.5	12.9	0.031	2.29	6.2	No apparent erosion
5	13.4	0.031	2.49	6.7	Large crack formed down the middle of the sample
0.5	13.4	0.035	2.20	6.8	No apparent erosion
0.5	13.6	0.036	2.17	6.9	Chunk of till dislodged from damaged corner
0.5	13.6	0.039	2.10	7.3	No apparent erosion
5	13.6	0.044	2.02	7.9	Chunk of till dislodged from corner, crack enlarged, mass erosion occurred as a chunk of till dislodged from the crack
2	13.6	0.046	2.00	8.2	Gravel pieces embedded in sample became more visible

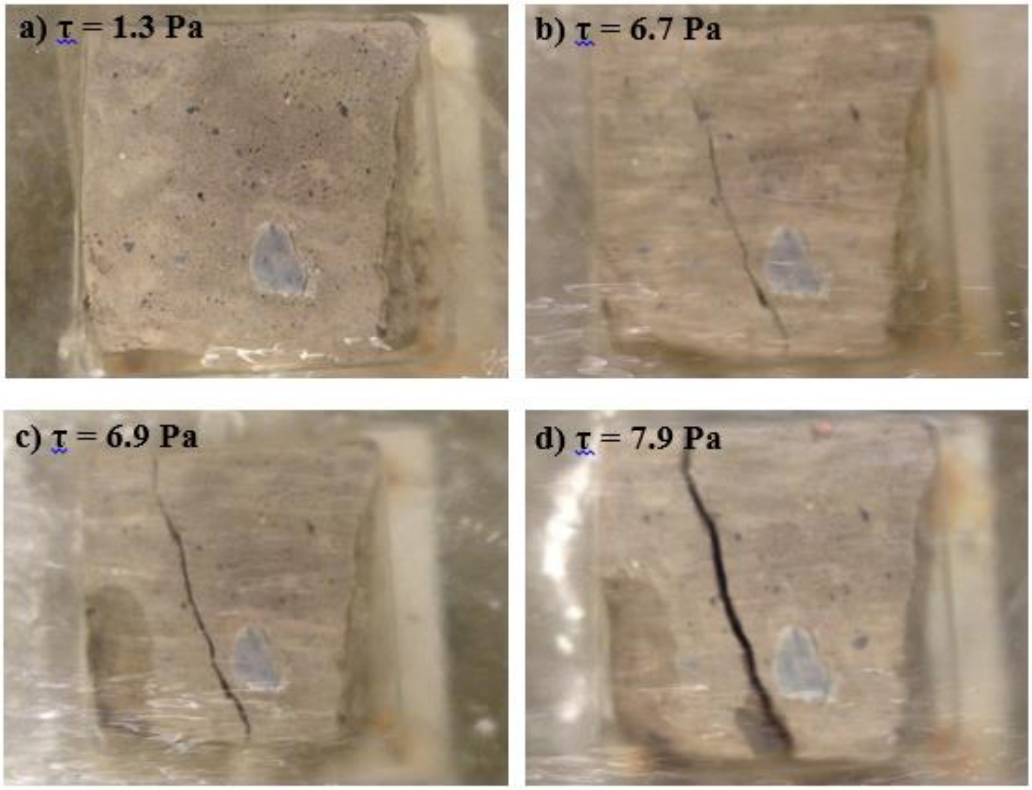

Figure 23: Sample 1 - progression of erosion

Figure 24: Sample 1 - before and after erosion, top) plan view, bottom) elevation view

5.3.3 Sample 2

Sample 2 was the second sample tested to determine the critical shear stress and erosion mechanism under natural moisture content and clear flow conditions. Erosion mainly occurred in the following pattern: first, cracking and delineating of chunks of till at irregularities in the surface, followed by mass erosion with the chunks of till dislodging and flowing downstream. At applied shear stresses ranging from 1.7 Pa – 6.1 Pa, erosion was not present except for corner and edge cracking from locations damaged during trimming of the sample. When the shear stress was increased to 6.7 Pa, very small gravel pieces eroded from the surface of the sample by first becoming more exposed and then dislodging from the surface. With a further increase to 7.6 Pa, cracks began forming along the surface, including a large crack from a large gravel piece to the edge of the sample. At 8.3 Pa, chunks of till began dislodging from the cracked areas, and this was taken to be the critical shear stress of the sample. As the applied shear stress increased to 8.8 Pa, more large cracks formed along the surface and the sample continued to undergo mass erosion. Similar to Sample 1, Sample 2 did not have an entirely flat surface when it went into the flume – one of the downstream corners underwent damage during cutting, and erosion in this area was not counted in the studies. Table 5 summarizes the flume tests and Figure 25 shows the progress of erosion over time. Figure 26 shows the sample before and after erosion.

Table 5: Sample 2 flume tests and observations

Duration (hrs)	Discharge (L/s)	Slope	Depth of Water (cm)	Shear Stress (Pa)	Observations
0.25	1.1	0.046	0.39	1.7	Small pieces broke off damaged corners
0.25	2.3	0.046	0.63	2.8	Till breaking off corners
0.25	3.2	0.046	0.75	3.3	Cracks formed near the edges
0.25	5.2	0.046	0.98	4.2	No apparent erosion
0.25	6.6	0.046	1.21	5.1	No apparent erosion
0.5	8.3	0.046	1.45	6.1	No apparent erosion
0.25	9.8	0.046	1.60	6.7	Very small gravel pieces popped out of surface
1	11.4	0.046	1.74	7.2	Large edge and corner pieces broke off
1	12.3	0.046	1.84	7.6	Cracks formed around edges and large crack from gravel piece to edge of sample
1	12.9	0.046	1.92	7.9	More cracks formed
2	13.2	0.046	2.02	8.3	Scouring occurred in cracks, pitting of the surface, cracks formed around gravel pieces, small gravel particles popped out of surface, mass erosion occurred as chunks popping out of cracks, taken as critical shear stress
3	13.6	0.046	2.10	8.6	Cracks enlarged
3.5	13.8	0.046	2.15	8.8	Cracks formed around gravel piece, corner of till fell off, large crack formed across the sample

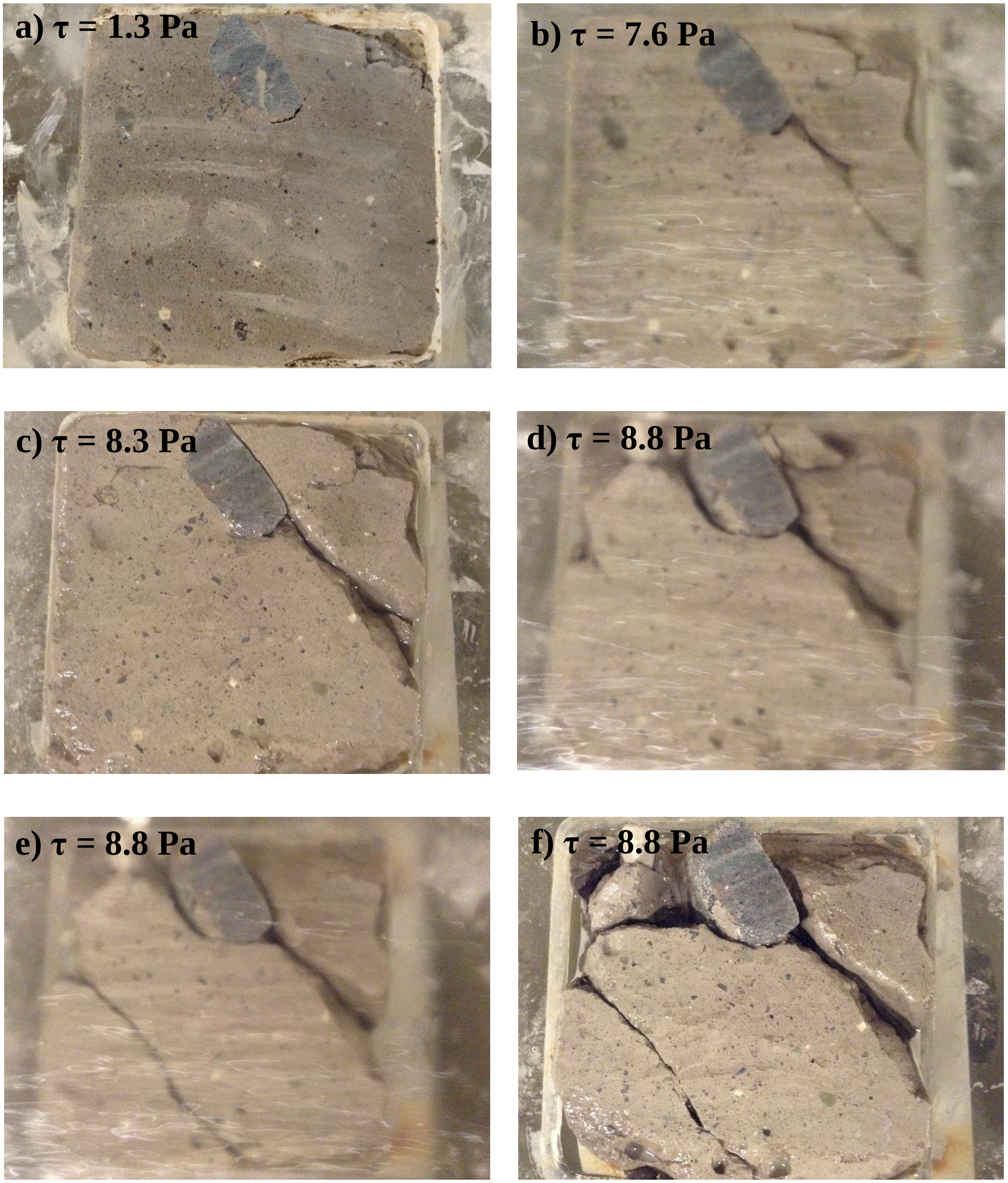

Figure 25: Sample 2 - progression of erosion

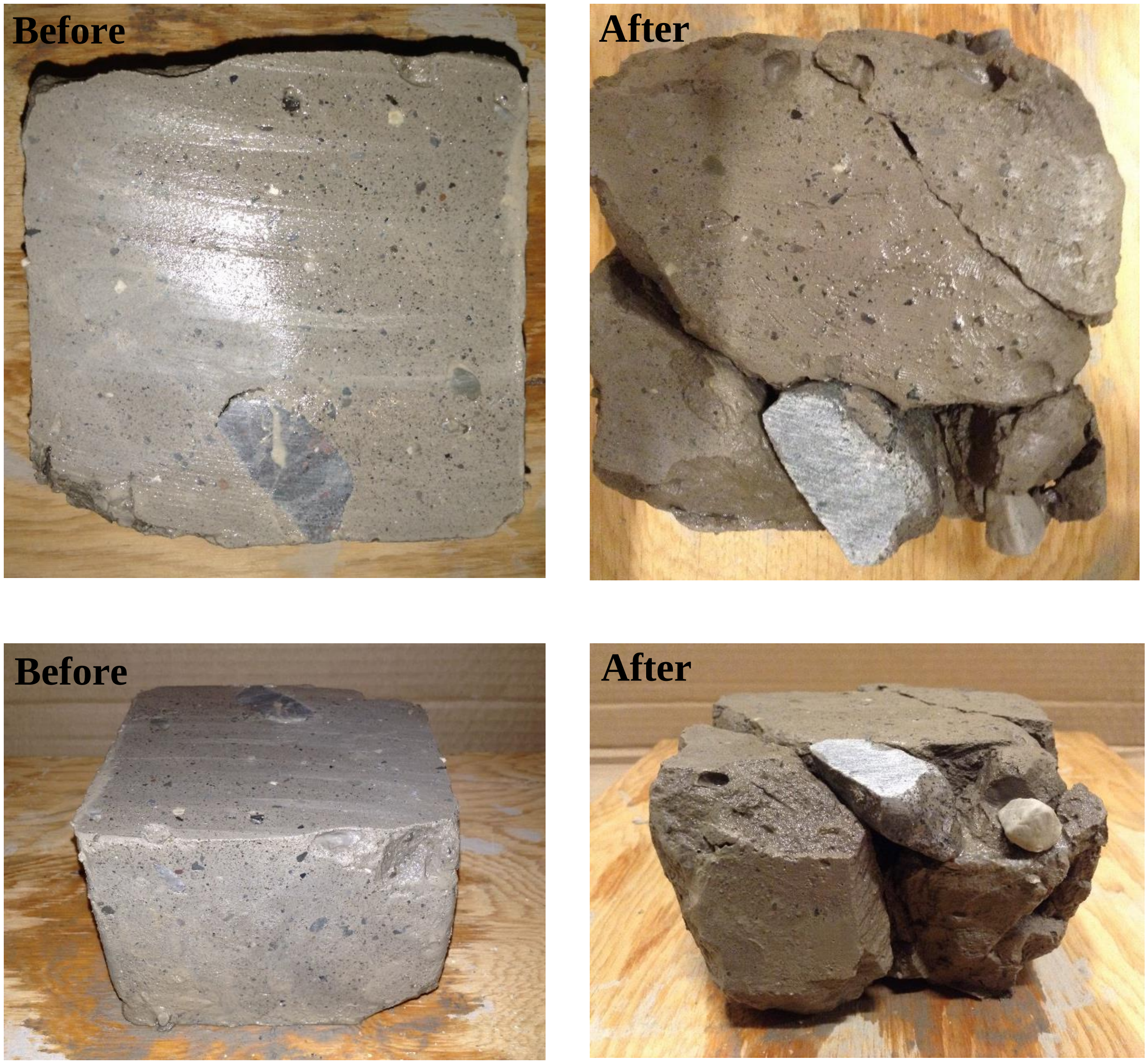

Figure 26: Sample 2 - before and after erosion, top) plan view, bottom) isometric view

5.3.4 Sample 3

Sample 3 was left to air dry for 48 hours after it was cut to determine the effect of drying on critical shear stress values. The test showed that drying had an extreme effect on erosion, with quick initiation, rapid progression, and a much lower critical shear stress value than Samples 1 and 2. When the sample was put into the flume, an initial shear stress of 1.2 Pa was applied. Details of the study are in Table 6. Surface erosion began immediately, with particles quickly eroding from the surface. The material eroded around large gravel particles embedded in the sample and erosion occurred predominately on the edges and corners of the sample. In a timeframe of thirty minutes, the sample had lost its structure and the test was stopped. The sample resulted in a slumped pile of material. The quick progression of erosion is shown in Figure 27, and an image of the sample before and after erosion is shown in Figure 28. 1.2 Pa was taken to be the critical shear stress for this sample. However, the critical shear stress could be lower as the minimum shear stress applicable is limited by the lower limit of shear stresses achievable in the flume.

Table 6: Sample 3 flume tests and observations

Duration (hrs)	**Discharge (L/s)**	**Slope**	**Depth of Water (cm)**	**Shear Stress (Pa)**	**Observations**
0.5	1.1	0.046	0.28	1.2	Major surface erosion, most of sample eroded and remaining sample lost shape and slumped

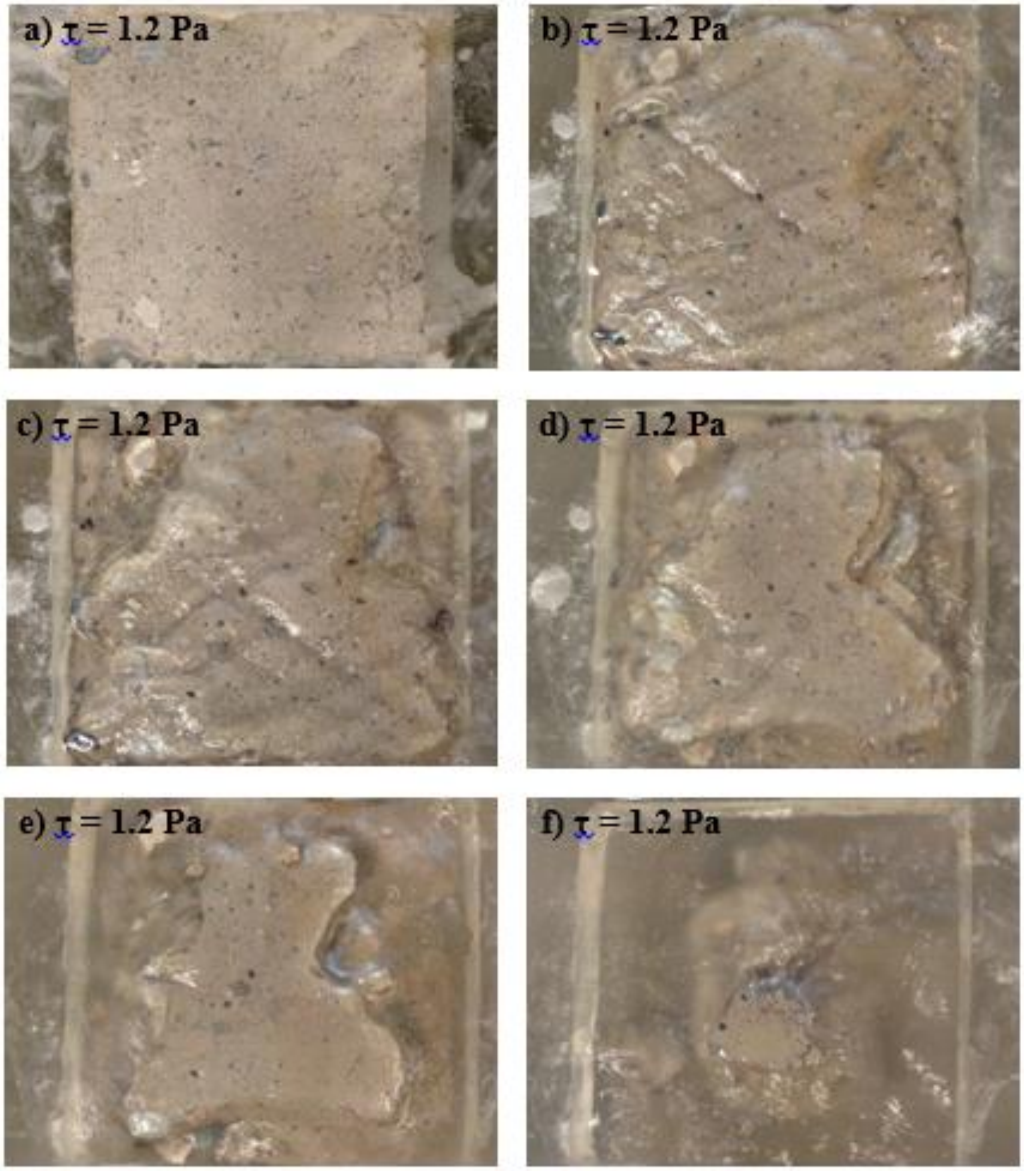

Figure 27: Sample 3 - progression of erosion

Figure 28: Sample 3 - before and after erosion, isometric view

5.3.5 Sample 4

Sample 4 was the second sample tested under air dried conditions to determine the effect of drying on the critical shear stress. The sample eroded quickly under a low shear stress. The applied shear stress began at the lowest possible in the flume: 0.9 Pa. Erosion began immediately, starting with surface erosion with particles on top quickly washing downstream and eroding around the gravel pieces present in the sample. The sample seemed to erode in very small cohesive chunks, not on a particle-by-particle basis, but not by large-scale mass erosion and cracking as seen in Samples 1 and 2. The test ran for one hour before the sample had completely lost its structure. The critical shear stress was taken to be 0.9 Pa, however, it may be lower than this because this is the minimum stress possible in the flume. Unlike the other samples, Sample 4 was not cut flat across the surface because the natural surface of the sample was already flat and cutting could have caused surface weakening or cracking. Table 7 summarizes the flume test and observations and Figure 29 shows the progression of erosion over time. Figure 30 shows an image of the sample before and after erosion.

Table 7: Sample 4 flume tests and observations

Duration (hrs)	Discharge (L/s)	Slope	Depth of Water (cm)	Shear Stress (Pa)	Observations
1	1.1	0.046	0.20	0.9	Major surface erosion around gravel particles, mass erosion, quickly eroded majority of sample and sample left lost shape and slumped

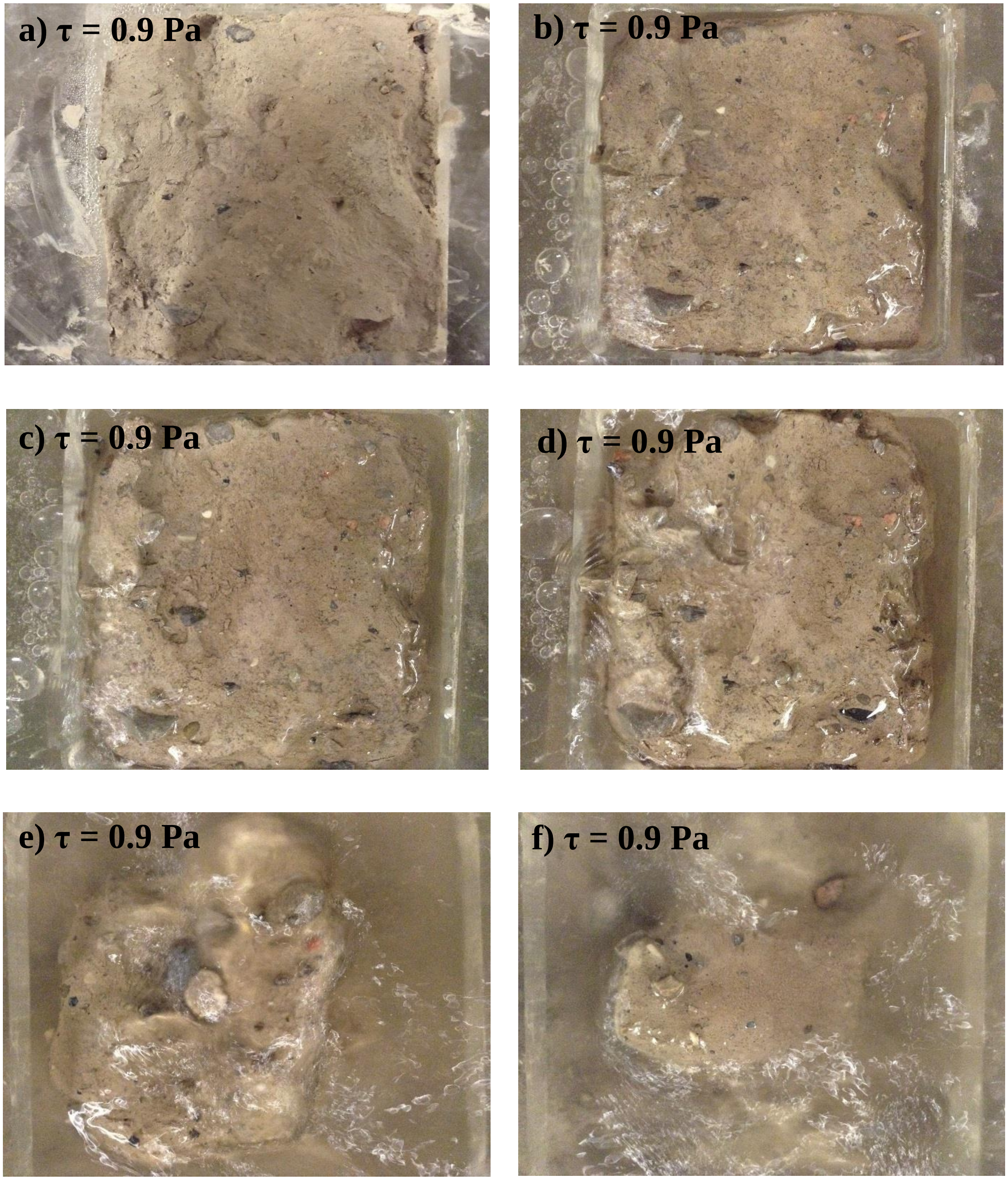

Figure 29: Sample 4 - progression of erosion

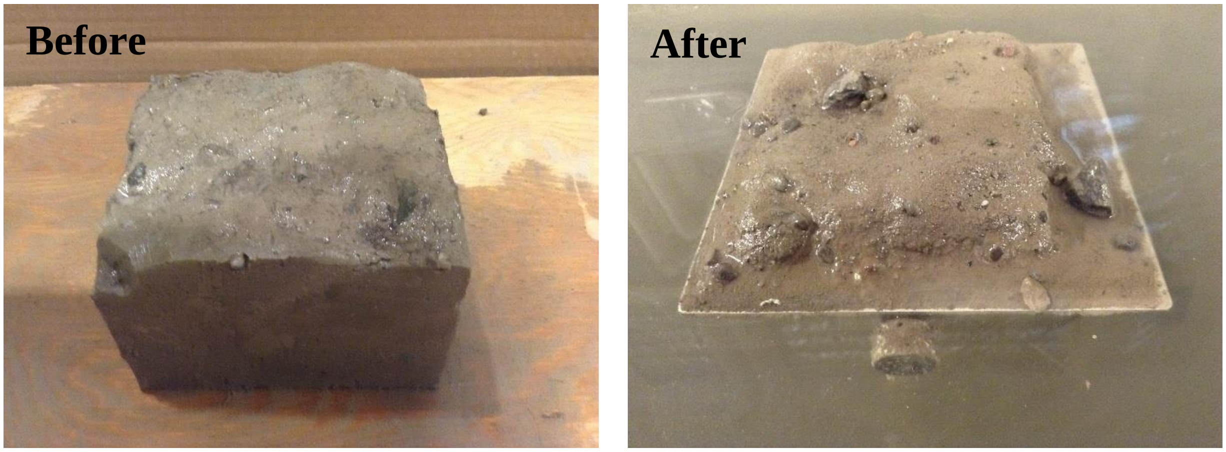

Figure 30: Sample 4 - before and after erosion, isometric view

5.3.6 Sample 5

Sample 5 was tested with 78 large gravel particles in the flow, with diameters ranging from 11 to 37 mm, to see the effect of large particle impact and that of the alluvial cover in the field. The gravel particles remained stationary upstream of the sample under low shear stresses. As the applied shear stress was increased, the gravel particles moved to cover the sample, and then eventually began rolling downstream, causing damage to the sample surface and initiating mass erosion. At first, the stationary gravel upstream of the sample caused increased water depth at the sample location, which increased the applied shear stress on the sample itself. When the applied shear stress was increased to approximately 4 Pa, the gravel particles moved downstream and covered the sample (Figure 31), making the assumed effective average shear stress on the sample unknown but assumed to be close to 0 Pa.

Figure 31: Stationary gravel particles on Sample 5

Erosion was not observed while the gravel particles covered the sample. When the average applied shear stress was increased to approximately 5 Pa, the gravel pieces moved a small amount on the sample causing corner damage, but then remained stationary. When the flow was increased to an average applied shear stress of 6.8 Pa, the gravel particles started rolling down the flume, and the sample began to form small cracks and erode through surface pitting. This was taken as the critical shear stress. Figure 32 shows an image of the gravel particles moving down the flume.

Figure 32: Sample 5 gravel particles moving downstream

Mass erosion then proceeded to occur on the downstream corner of the sample due to cracks caused by impacts from the gravel particles. When cracks formed in the sample, the impact of the gravel particles enlarged the cracks at a faster pace than the clear flow conditions did. The impacts from the gravel particles also caused a noticeable increase in incision of the surface by pitting and subsequent smoothing of the surface as compared to clear flow conditions. A summary of the flume tests and observations is given in Table 8. A progression of the erosion is shown in Figure 33. Figure 34 shows the sample before and after erosion where it is clear that the upstream end of the sample experienced more incision than the downstream end of the sample.

Table 8: Sample 5 flume tests and observations

Duration (hrs)	Discharge (L/s)	Slope	Depth of Water (cm)	Shear Stress (Pa)	Observations
0.5	1.0	0.046	0.32	1.4	Gravel remained stationary upstream, no erosion
0.25	1.6	0.046	1.01	4.3	Gravel moved slightly causing increased depths, no erosion
0.5	5.3	0.046	2.15	0	Gravel covered sample, some smaller pieces rolled downstream, no apparent erosion
1	6.6	0.046	2.35	0	Gravel cover remained mainly stationary, small gravel movement caused corner damage, no other erosion
1	8.7	0.046	1.62	6.8	Gravel cover no longer remained stationary, abrasion caused corner damage, surface pitting, small cracks formed
1	10.2	0.046	1.7	7.1	Gravel pieces embedded in sample started popping out
0.25	11.7	0.046	1.82	7.5	Erosion on edge of sample due to abrasion, gravel pieces popping out of center of sample
1.25	11.7	0.046	1.94	8.0	Large edge and corner piece broke off, major cracking occurred and quickly enlarged by abrasion, mass erosion occurred from cracks, incision in upstream end of sample from abrasion, pitting and smoothing of the surface
2	12.4	0.046	2.01	8.2	Mass erosion and incision continued to occur
4	12.9	0.046	2.17	8.8	Mass erosion and incision, especially at upstream edge of sample, continued to occur

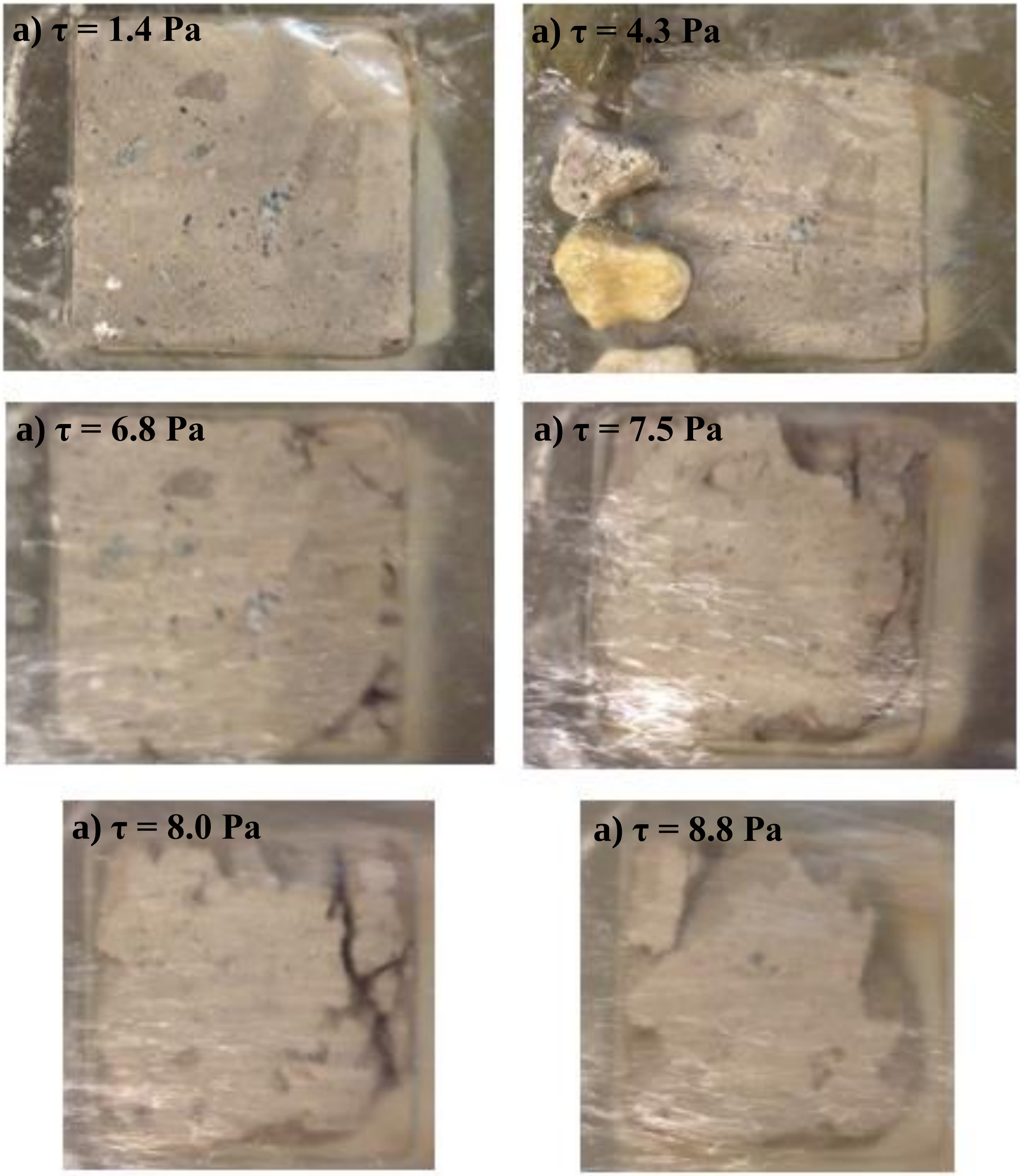

Figure 33: Sample 5 - progression of erosion

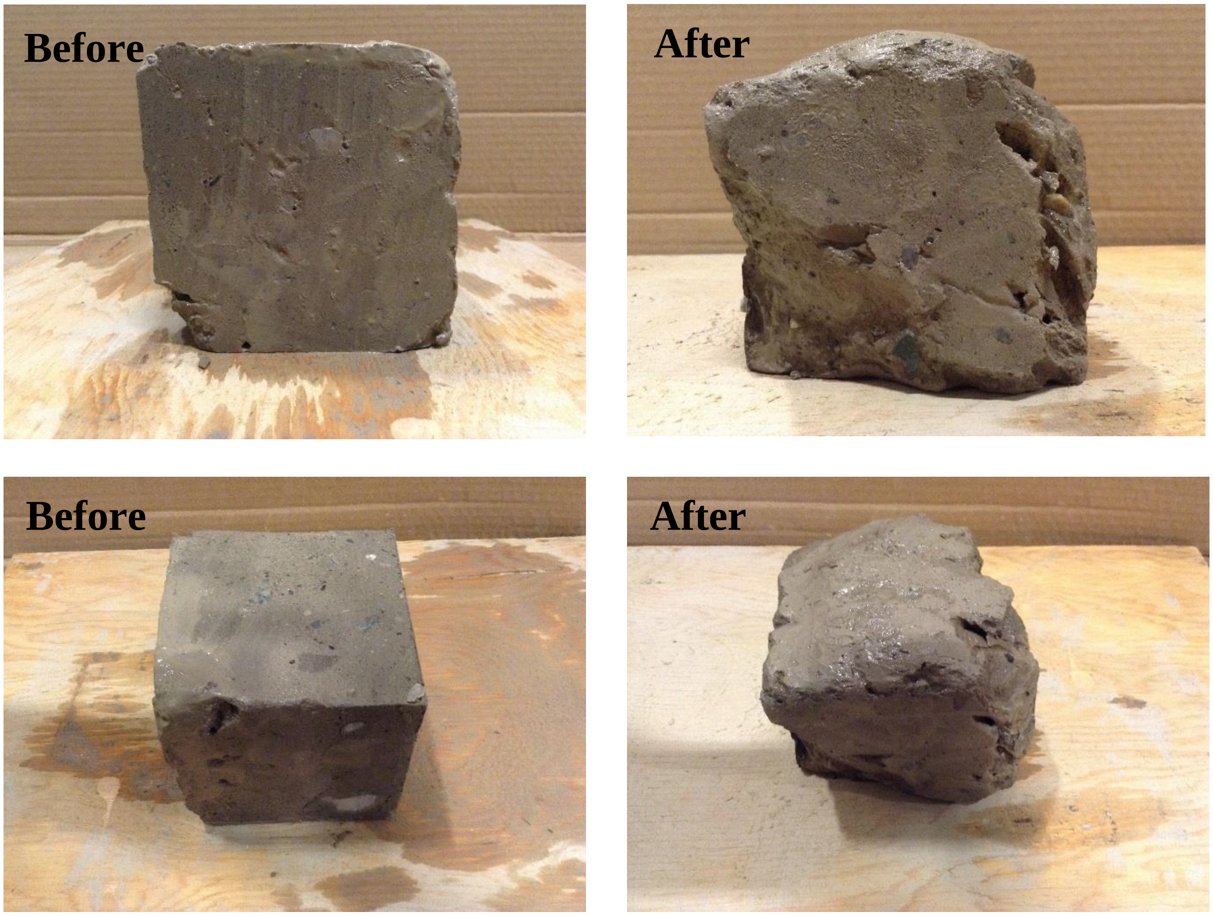

Figure 34: Sample 5 - before and after erosion, top) elevation view, bottom) isometric view

5.3.7 Sample 6

Sample 6 was the second sample tested with the same distribution of gravel particles present in the flume. Similar to Sample 5, the gravel particles remained stationary at first, then moved to cover the sample as flows increased, eventually causing damage due to impacts on the sample surface once the gravel started rolling downstream. When the applied critical shear stress was less than 3 Pa, the gravel particles did not move in the flume and remained upstream of the sample, shown in Figure 35. However, the gravel caused an increase depth of water over the sample, thus, an increase in the applied shear stress on the sample. Erosion was not observed under these flow conditions.

Figure 35: Sample 6 gravel placement with flow < 4.5 L/s

Once the critical shear stress was at approximately 3 Pa the gravel slowly moved down the channel and eventually covered the sample, varying the applied shear stress from an assumed 0 Pa when the sample was covered, to 8.2 Pa, when the sample was uncovered. Figure 36 shows the gravel before it moved downstream and after it moved downstream and covered the sample.

Figure 36: Sample 6 gravel placement with flow = 4.5 L/s

When the applied shear stress was increased to approximately 4.3 Pa, the gravel pieces slowly moved down the channel, but the gravel on the sample remained on the sample for the majority of the testing period before eventually moving off the sample. Once the gravel left the sample surface and rolled downstream, it was apparent that erosion had occurred on the sample while the gravel was covering it. Thus, for this sample, only a range for the critical shear stress value could be determined. The range of the critical shear stress value is 4.3 – 6.1 Pa since 4.3 Pa was the previous known applied shear stress value where erosion was not seen and 6.1 Pa was the known applied shear stress value where erosion was seen. When the average shear stress was increased to approximately 7.9 Pa, the gravel no longer stayed on the sample and quickly rolled downstream. For these higher flow conditions, the rolling gravel caused the sample to erode more quickly by first cracking, then delineating into chunks, and eventually undergoing mass erosion. It was observed that chunks would erode from the sample, causing irregularities in the surface of the sample, but the gravel particles would then smooth the surface. This phenomenon is evident in comparing Figure 37e and Figure 37f. A summary of the flume tests and observations is given in Table 9, and the progression of erosion is pictured in Figure 37. Figure 38 shows images of the sample before and after erosion, where it is evident that the major erosion occurred on the corners and edges of the sample. However, Figure 39 is a close-up image of the surface of the sample which shows erosion that occurred in the center of the sample in the form of pitting and small-scale mass erosion. Additionally, worm holes were observed within the exposed areas after erosion occurred on the downstream end of the sample, which are pictured in Figure 40.

Table 9: Sample 6 flume tests and observations

Duration (hrs)	Discharge (L/s)	Slope	Depth of Water (cm)	Shear Stress (Pa)	Observations
0.5	2.0	0.046	1.23	5.2	Gravel stationary upstream, caused increase in water depth and higher shear stress. Erosion not observed.
0.5	3.2	0.046	0.99	4.3	Gravel moved slightly, remained upstream, decreased water depth above sample - lowered applied shear stress, no apparent erosion.
0.5	4.5	0.046	2.00	0 - 8.2	Gravel slowly moved, caused increase in water depth above sample. Gravel then moved to cover sample entirely - protected sample from shear stress.
3	6.3	0.046	2.50	0 - 10.0	Gravel slowly moved down channel, but some remained covering sample. While gravel was covering sample, grooves appeared in the sample downstream of the rocks and mass erosion occurred.
1	8.4	0.046	1.45-2.08	6.1 - 8.5	Gravel covered sample and eventually moved revealing mass erosion that had occurred on the sample. Erosion occurred while gravel was covering the sample.
1	10.4	0.046	1.73	0 - 7.2	Gravel remained on top of sample, no additional erosion.
1	11.6	0.046	1.91	7.9	Gravel began rolling downstream - caused corner damage and mass erosion. Cracks formed, abrasion caused gouges in the center of the sample. Chunks delineated and eroded around protruding gravel.
2	12.1	0.046	1.99	8.2	Large chunks fell off near cracked corner areas and center chunks popped out of surface and eroded.
2	12.9	0.046	2.08	8.5	Gravel pieces rolling quickly over sample seemed to cause increased smoothing and incision.
3	13.2	0.046	2.11	8.6	Small gravel pieces embedded in sample popped out of the center, abrasion due to rolling gravel caused a smoothing of the surface.

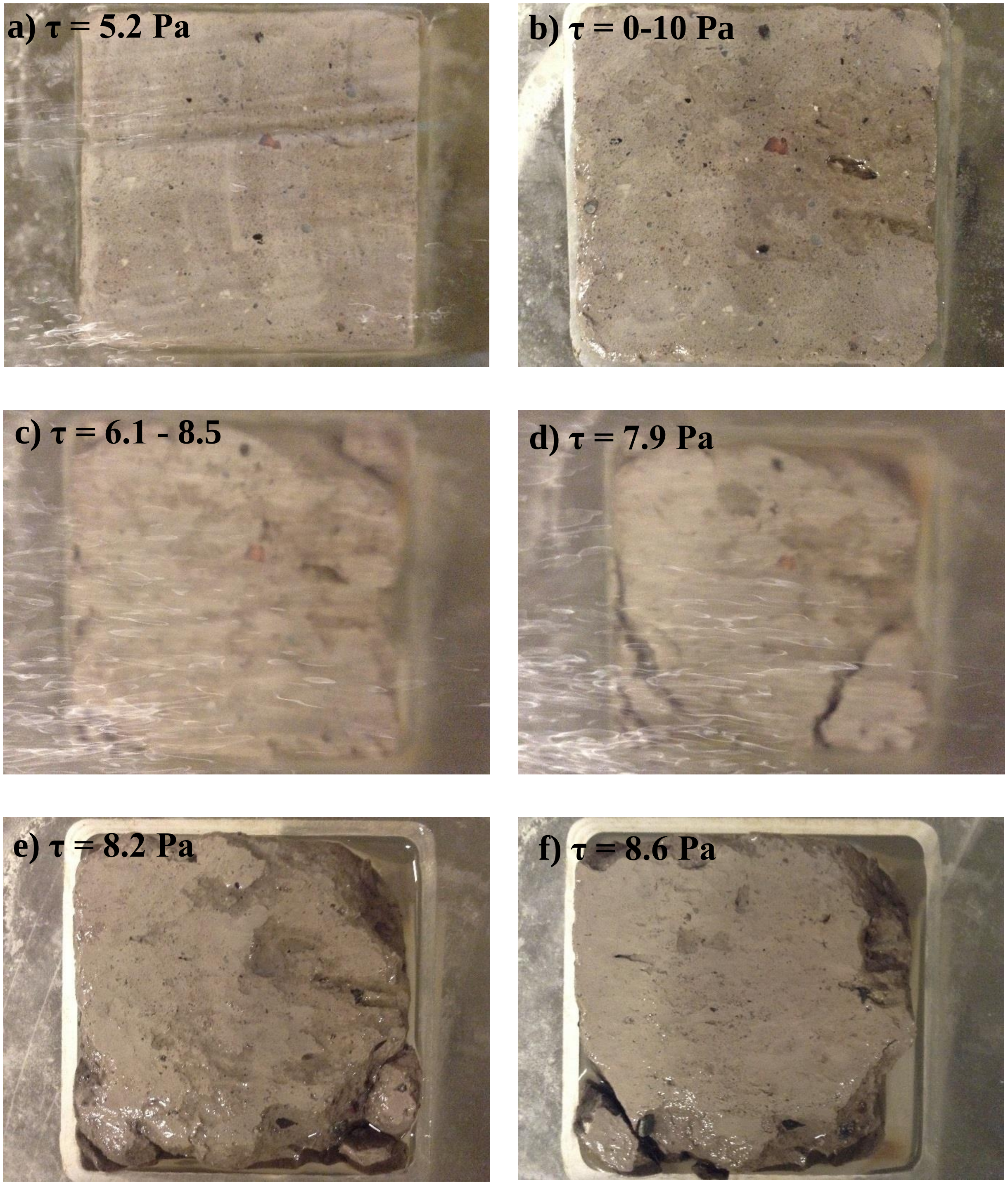

Figure 37: Sample 6 - progression of erosion

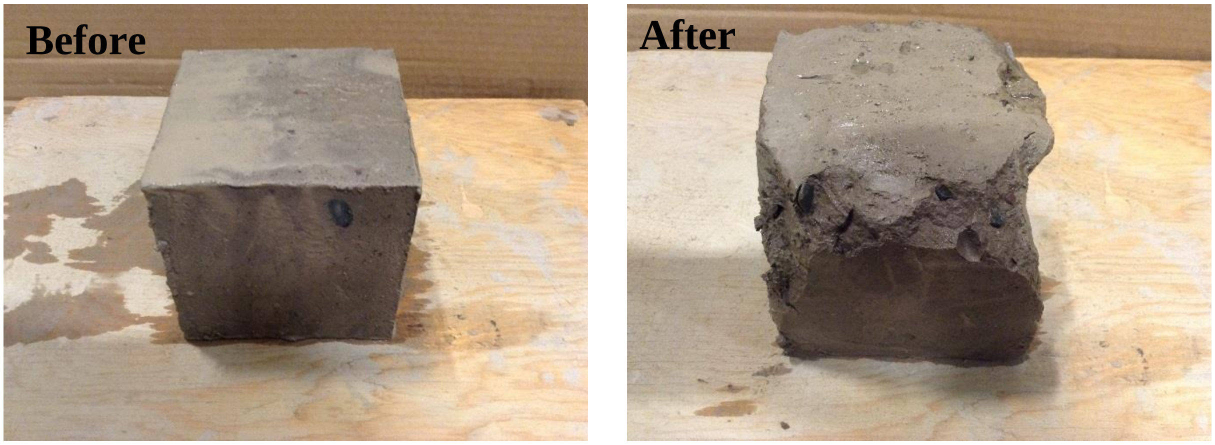

Figure 38: Sample 6 - before and after erosion, isometric view

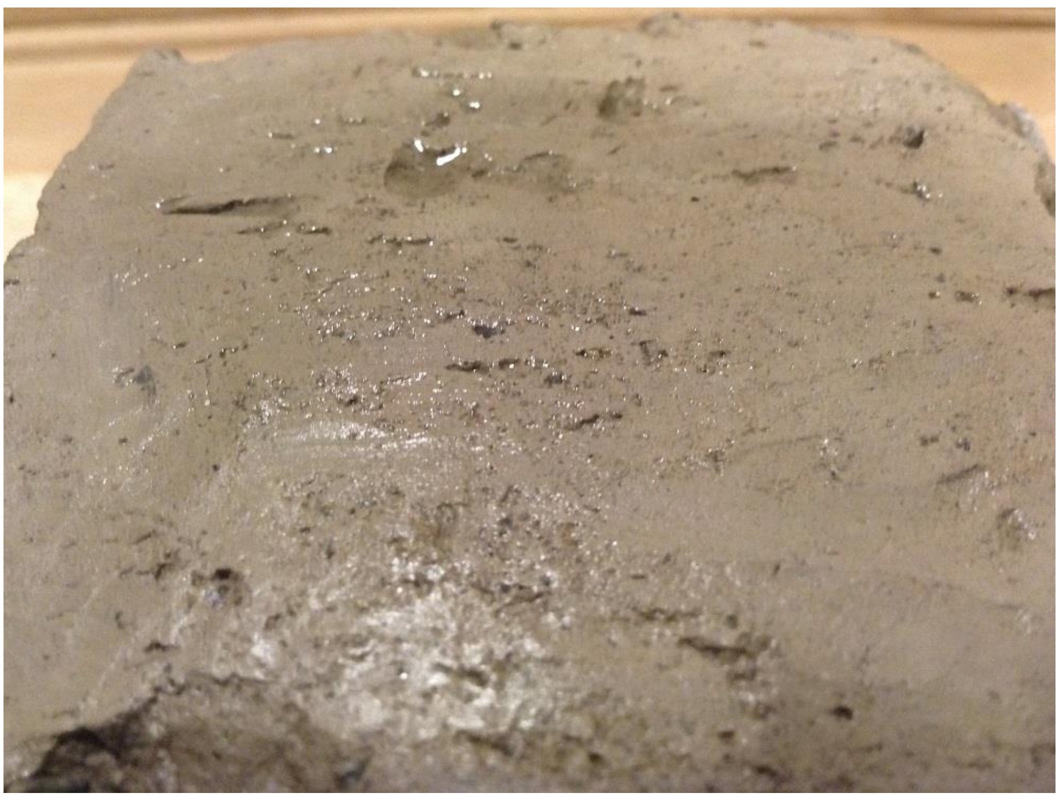

Figure 39: Sample 6 - close-up of erosion on surface

Figure 40: Sample 6 - erosion showing worm holes

6.0 Discussion

The field observations and flume tests performed on the till samples of Medway Creek made the natural "structuration" of the till apparent and confirmed that mass erosion is the dominant erosion mechanism. The "structuration" of the material, as termed by Lefebvre et al. (1985), was readily apparent throughout the field visit, and the handling and testing of the material. The material would fracture across planes within the sample, and in some cases these fractures extended all the way through the sample (see Figure 24). The fractures often developed near gravel particles embedded in the sample, but other times there was no apparent origin, indicative of an existing plane of weakness within the sample. These observations are similar to those from some previous studies (Kamphuis et al. (1990); Mier and Garcia (2011); Gaskin et al. (2003); Lefebvre et al. (1985)) in which the till eroded by blocks of clay delineating and breaking off from the sample, usually around discontinuities or areas of weakness. However, erosion is not immediate once critical stresses are achieved because erosion (removal of pieces of till) is preceded by a phase of fracturing. Unlike some previous studies (Kamphuis et al. 1990; Gaskin et al. 2003; Mier and Garcia 2011), the erosion rate did not always decrease over time at a given applied shear stress. Instead, cracks formed immediately, then slowly widened over time, leading eventually to the delineation of chunks of till and mass erosion. In this sense, the initial fracturing of the sample would happen quickly, but most of the erosion occurred after a relatively long delay related to crack propagation and widening. At a given shear stress there was only one phase of crack propagation and mass erosion, after which erosion ceased.

While mass erosion was the dominant erosion process in the till, surface erosion had an important role. In the flume studies, small gravel particles would dislodge from the surface by first becoming slightly uncovered due to lowering of the till surface by hydraulic erosion, similar to the surface erosion observed by Mier and Garcia (2011). Once uncovered and dislodged from the sample, the new irregularities in the sample surface would initiate mass erosion. The amount of surface erosion that occurred was less than a centimeter, but it played a significant role in exposing gravel pieces and therefore in the whole erosion process.

The distribution of particle sizes within till material influences the erosion processes and susceptibility. The particle-size distribution of the till material shows a wide range of particle sizes, as expected. The particle size distributions of the three samples were very similar, which is most likely due to the close proximity of the sample locations. The range of particle sizes within the till impacts the entire erosion process—the smallest particles (silt and clay) create the cohesive nature, and the largest particles cause areas of physical weakness where cracking and erosion is often initiated. The initiation of erosion around gravel particles was observed during the laboratory flume tests of this study, similar to past studies (Kamphuis et al. 1990; Gaskin et al. 2003; Mier and Garcia 2011). The particle size distribution tests performed on the three samples for this study were limited by the size of the sample tested which did not allow for any gravel particles larger than the sample itself. The boulders that are present within the till material *in* situ could not be captured in the particle size distribution, but it is likely that their effect on erosion initiation is similar to other gravel particles but on a much larger scale.

The critical shear stress value for till at its natural moisture content with clear flow conditions was determined to be approximately 8 Pa, which is generally higher than values in previous tests. Kamphuis et al. (1990) and Mier and Garcia (2011) both found lower critical shear stress values (0.65-4.1 Pa for Kamphuis et al. (1990) and 4.2 Pa for Mier and Garcia (2011)) for their tested clay and till samples, with two of the samples by Kamphuis et al. (1990) an order of magnitude less. The difference can be attributed to the wide variation of clay and till properties in general.

However, the critical shear stress values are within the range of values determined by Gaskin et al. (2003) for Champlain Sea Clay, albeit a wide range is given. Although the critical shear stress values from the two *in situ* jet-tester tests are similar in magnitude, whether they are a true representation of the real critical shear stress is in question due to the nature of the test. The critical shear stress was determined by the conditions at the time when the first chunk of material became dislodged from the sample. As discussed above, mass erosion stems from the natural structure of the cohesive material matrix and irregularities in the surface. Therefore, tests that do not allow the progression of erosion to occur, such as jet testers, will not get an accurate representation of what shear stress causes the initiation of erosion. The flume test did allow the sample material to go through the erosion cycle, and it also more accurately represented real flood conditions by having a flow rate, and thus, shear stress value, that slowly increased over time, making the obtained critical shear stress values more reliable.

Physical weathering of the material by air-drying the sample before testing decreased the critical shear stress value significantly and had extreme effects on the erosion process. The reduced critical shear stress, from around 8 Pa in normal moisture content conditions, to less than 1 Pa under the air-dried condition, is in agreement with the Gaskin et al. (2003) study on the effect of drying Champlain Sea Clay. There were no visible cracks within the sample during or after the drying process, but micro-fissures may have formed within the sample. This was evident when flume testing began and mass erosion occurred quickly in the form of very small chunks of till breaking away from the surface. Microfissuring was apparent along the dried banks of the river on the field site, and can be seen in Figure 14. Microfissuring seemed to penetrate 15 cm in the field (Figure 14) and in air-dried samples, which increased the erodibility of the material. The sample eroded around large gravel particles embedded in the sample, which is also observed in the field in Figure

14. It was clear from the final slumped nature of the material after flume testing that the samples had lost their cohesive structure after weathering. This is in agreement with the study by Govers and Loch (1992) where a lower initial water content led to more microfissuring and less resistance to erosion due to a weakening of the cohesive nature of the material. The extreme effects that drying has on the erodibility of till put the lower banks of till rivers in the greatest danger of erosion. These areas are exposed to the most frequent wetting-and-drying cycles from changing river stages. The increased frequency and intensity of storms due to climate change also puts the lower and mid-banks at risk of increased erosion.

The presence of alluvial gravel during laboratory flume tests increased the erosion of the till sample, and decreased the critical shear stress from about 8 Pa to less than 7 Pa, which agrees with a decrease in critical shear stress due to abrasion that was concluded by Kamphuis et al. (1990) in a study about abrasion due to sand. The impacts from the gravel particles eroded the till sample and subsequently smoothed the surface. This process inhibits the formation of local bed topography, which agrees with the conclusion by Hrytsak (2012) that till is too soft a material to form local topography. The smoothing of the surface was dissimilar to past bedrock studies where deep, local incisions were created by focused abrasion in grooves and pits, and highlights the difference between semi-alluvial bedrock rivers and semi-alluvial till rivers (Sklar and Dietrich 2004; Johnson and Whipple 2007; Chatanantavet and Parker 2008). The gravel particles also caused considerable surface waves while they were on top of the sample, and in some cases this caused additional erosion. This phenomenon may be specific to the laboratory test since the size of the gravel particles was large relative to the depth of the water. However, this could mean that large boulders or debris, such as fallen trees, within the river may cause erosion due to additional turbulence and thus, high localized shear stress values. The test did not provide adequate means to look at the movement of the alluvial cover over a till surface since the till sample was too small in size and the majority of the gravel particle movement occurred on a smooth plexiglass surface that is not representative of the natural friction of a till river bed.

The semi-alluvial nature of Medway Creek was apparent in the field visit. There was an extensive alluvial cover along the banks of the river (Figure 17) and intermittent covering of the till in the bed of the river observed during the field visit, which was also observed at Medway Creek by Hrytsak (2012). Throughout the laboratory flume tests, gravel particles would become dislodged from the till sample and move downstream, either within the flow or by saltating, depending on the size of the particle. This reinforces the semi-alluvial aspect of till rivers where the till itself provides the alluvial material. An increase in applied shear stress has shown an increase in erosion. Thus, during peak flows, more gravel particles will become dislodged from within the till due to erosion. Gravel particles are especially likely to originate from the lower banks of the river that experience a higher amount of erosion due to weathering from the wetting-and-drying cycle. The semi-alluvial aspect of till rivers influences the geomorphology of the river itself due to supplying the alluvial material that can subsequently protect or erode the till material.

The flume test was advantageous compared to a jet-tester because it allowed for mass erosion, and erosion on a larger scale in general. The sample collection process, methodology, and observations, all allowed for valuable research to develop from this study. However, there are ways in which the process could be improved. In collecting the sample, it would be ideal to have larger chunks extracted directly from the bed or the banks in order to have more samples to test and a better likelihood of the *in situ* conditions of the sample to be retained. Testing more samples would allow for better understanding of both the average and the range of behavior of the material. This would require the use of excavating equipment, which was not allowed at the particular study location, but which may be used at similar sites and future studies. The collection of the alluvial cover sample could have been improved by collecting a larger sample size to have a bigger range of gravel sizes to see the impact the various sizes have on erosion. The flume test could be improved by using a larger-sized sample to allow for larger-scale mass erosion to develop, which would also decrease any effect that edge or corner damage may have on erosion initiation. Using a flume that allows for higher shear stress values would be helpful to see what the impact of a further increase in applied shear stress has on the material erosion. A larger flume might also allow for a comparison of subcritical and supercritical flow. In collecting data and taking observations, it would be ideal to have a video, or a time-lapse photo series, of the fracturing and erosion process as it occurs in order to better capture the erosion process for analysis.

River engineering works in till rivers will be most effective if they closely mimic naturally occurring features. Whenever installing river engineering works, erosion control needs to be addressed, and studying the erosion mechanisms of till rivers is the best way to establish how erosion occurs and what natural factors influence it. Knowing the critical shear stress of the bed material can aid in preventing erosion by designing channels that reduce the likelihood that the shear stress will exceed the critical value. This study estimated the critical shear stress of till rivers in southern Ontario to be around 8 Pa, which means that channels designed in similar rivers should aim for a maximum shear stress that is below this value to ensure erosion does not occur. Of particular concern are the banks that are exposed to wetting-and-drying cycles. Engineered ways to dissipate the energy of the river before the shear stress from the water is applied to the banks is an effective way in mitigating bank erosion. A few ways to dissipate energy are to create pools and backwater, or riffles in lower gradient rivers, and vortex rock weirs in higher energy systems. Using vegetation along the banks, and even under bridges, will decrease local shear stress values and help mitigate erosion. The addition of a gravel layer in this particular study showed a decrease in the critical shear stress, which means that a gravel "protection" layer as an engineered means to prevent erosion may actually increase the erosion of the channel. To protect the till, there may need to be a minimum cover depth in order for the gravel to remain stationary and not allow local turbulence to reach the till itself. In all engineering works, it is key to monitor what has been constructed, and modify the design as needed.

7.0 Conclusions and Future Work

The objectives of this study were to observe the mechanisms of till erosion and determine a value of the critical shear stress of till, specifically the till found at Medway Creek in southern Ontario, and to understand how the alluvial cover impacts till erosion. Samples were collected from Medway Creek in London, ON, and tests were carried out in a hydraulic flume in the McGill University Hydraulics Lab in Montreal, QC. The main findings are summarized below:

1. The critical shear stress of till taken from Medway Creek was determined to be approximately 8 Pa. This value is greatly reduced when the material is subjected to physical weathering in the form of wetting-and-drying. Air-dried samples were determined to have a critical shear stress < 1 Pa.
2. The till material had an apparent internal structure, which led mass erosion to be the dominant form of erosion. Mass erosion initiated around irregularities and planes of weakness within the internal structure, especially around embedded gravel particles. Mass erosion generally occurred in the following sequence: delineation of chunks of till, often around gravel particles or irregularities, followed by a widening and deepening of fractures, leading to an eventual dislodging of chunks of till which then eroded downstream.
3. The presence of an alluvial cover in the form of a single layer of gravel particles lowered the critical shear stress value to less than 7 Pa. Saltating gravel particles impacted the sample and created areas of weakness for mass erosion to take place. When the gravel particles remained stationary and covered the till, turbulence around the gravel created localized high areas of shear stress which eroded the sample. However, this phenomena could be particular to the testing environment and may not be the case in the natural

environment. Gravel particles which saltated across the sample caused both incision and a smoothing of the surface.

Further research on this topic could include how vegetation impacts the critical shear stress of till, examining both naturally occurring vegetation, and vegetation that is often used in river engineering works, for both till at its natural moisture content, and till that has been air-dried. An assessment of depth of cover that may protect till rather than enhance erosion would be insightful in how to use gravel covers in erosion prevention. Additionally, future work could assess how an alluvial cover may influence the erodibility of air-dried till, as there was often an alluvial cover along the exposed banks of Medway Creek. These suggestions would allow for a better understanding of till exposed to wetting-and-drying, which appears to be the till most vulnerable to erosion.

References

Ashmore, P., and Church, M. (2001). The impact of climate change on rivers and processes in Canada. Available from the Geological Survey of Canada, Ottawa, Ont. Bulletin 555.

Coops, H., Geilen, N., Verheij, H. J., Boeters, R., and Van der Velde, G. (1996). Interactions between waves, bank erosion and emergent vegetation: an experimental study in a wave tank. *Aquatic Botany*, 53, 187–198.

Chapman, L.J. and Putnam, D.F. (1984). The Physiography of Southern Ontario, Third Edition [Data file]. Retrieved from http://www.geologyontario.mndm.gov.on.ca/mndmaccess/mndm_dir.asp?type=pub&id=MRD228.

Chatanantavet and Parker (2008). Experimental study of bedrock channel alluviation under varied sediment supply and hydraulic conditions. *Water Resources Research,* 44, 1-19.

Chatanantavet and Parker (2009). Physically based modeling of bedrock incision by abrasion, plucking, and macroabrasion. *Journal of Geophysical Research*, 114, 1-22.

Davidson-Arnott, R. G. D. and Langham, D. R. J. (2000). The effects of softening on nearshore erosion of a cohesive shoreline. *Marine Geology*, 166, 145-162.

Debnath, K., Nikora, V., and Elliott, A. (2007). Stream bank erosion: in situ flume tests. *Journal of Irrigation and Drainage Eningeering,* 133, 256-264.

Dreimanis, A. (1976). Tills: their origin and properties. In R. F. Legget (ed.), *Glacial Till (pp. 39).* Ottawa, ON: The Royal Society of Canada.

Foster, G. E. (1998). *Morphology of three semi-alluvial stream channels in southern Ontario.* (Master's thesis). The University of Western Ontario, London, ON.

Gaskin, S. J., Pieterse, J., Al Shafie, A., and Lepage, S. (2003). Erosion of undisturbed clay samples from the banks of the St. Lawrence River. *Canadian Journal of Civil*

Engineering, 30, 585-595.

Goulter, I. C. and Myska, N. M. (1987). The human component in flood warning and flood response system. *GeoJournal*, 15**:** 297–305.

Govers, G., and Loch, R.J. (1993). Effects of initial water content and soil mechanical strength on the runoff erosion resistance of clay soils. *Australian Journal of Soil Research,* 31: 549–566.

Grabowski, R. C., Droppo, I. G., and Wharton, G. (2011). Erodibility of cohesive sediment: The importance of sediment properties. *Earth-Science Reviews*, 105: 101-120.

Hanson and Cook (1997). Development of excess shear stress parameters for circular jet testing. *Proceedings of the 1997 ASAE Annual International Meeting*, Paper No. 972227.

Houwing, E. J. and van Rijn, L. C. (1998). In Situ Erosion Flume (ISEF): determination of bed shear stress and erosion of a kaolinite bed. *Journal of Sea Research*, 39: 243-253.

Hrytsak, T. (2012). *Alluvial cover dynamics in a semi-alluvial channel: a case study of Medway Creek, London, ON.* (Master's thesis). The University of Western Ontario, London, ON.

Johnson, J. P. and Whipple, K. X. (2007). Feedbacks between erosion and sediment transport in experimental bedrock channels. *Earth Surface Processes and Landforms*, 32, 1048-1062.

Julian, J. P. and Torres, R. (2006). Hydraulic erosion of cohesive riverbanks. *Geomorphology*, 76, 193-206.

Kamphuis, J.W. and Hall, K.R. (1983). Cohesive material erosion by unidirectional current. *ASCE Journal of Hydraulic Engineering*, 109, 49-61.

Kamphuis, J.W. (1983). On the erosion of consolidated clay material by a fluid containing sand. *Canadian Journal of Civil Engineering*, 10, 223–231.

Kamphuis, J.W., Gaskin, P.N., and Hoogendoorn, E. (1990). Erosion tests on four intact Ontario clays. *Canadian Geotechnical Journal*, 27, 692–696.

Khan, I. and Kastaschuk, R. (2011). Erodibility of cohesive glacial till bed sediments in urban stream channel systems. *Canadian Journal of Civil Engineering*, 38, 1363-1372

Krishnappan, B. G., and Droppo, I. G. (2006). Use of an *in situ* flume for measuring stability of sediment deposits in Hamilton Harbour, Canada. *Water, Air, and Soil Pollution: Focus*, 6, 557-567

Krone, R.B. (1999). Effects of bed structure on erosion of cohesive sediments. *ASCE Journal of Hydraulic Engineering*, 125, 1297–1301.

Kundzewicz, Z. W. and Takeuchi, K. (1999). Flood protection and management: quo vadimus? *Journal of Hydrological Sciences*, 33, 37–41.

Lefebvre, G., Rohan, K., and Douville, S. (1985). Erosivity of natural intact structured clay: Evaluation. *Canadian Geotechnical Journal*, 22, 508–517.

Lefebvre, G., Rohan, K., and Milette, J.P. (1986). Erosivity of intact clay: Influence of the natural structure. *Canadian Geotechnical Journal*, 23, 427–434.

Mehta, A. J., Hayter, E. J., Parker, W. R., Krone, R. B., Teeter, A. M. (1989). Cohesive Sediment Transport. I: Process Description. *Journal of Hydraulic Engineering*, 115, 1076-1093.

Meshkova, L. V, Carling, P. A., and Buffin-Belanger, T. (2012). Nomenclature, complexity, semi-alluvial channels and sediment-flux-driven bedrock erosion. In M. Church, P. M. Biron, and A. Roy (eds.), *Gravel-bed Rivers: Processes, Tools, Environments (pp. 424 432).* John Wily & Sons, Ltd.

Mier, J. M., and Garcia, M. H. (2011). Erosion of glacial till from the St. Clair River (Great Lakes basin). *Journal of Great Lakes Research*, 37, 399-410.

Raudkivi, A. J. (1998). *Loose Boundary Hydraulics.* Rotterdam, The Netherlands: A. A. Balkema.

Shugar, D., Kostaschuk, R., Ashmore, P., Desloges, J. and Burge, L. (2007). In situ jet-testing of the erosional resistance of cohesive streambeds. *Canadian Journal of Civil Engineering*., 34, 1192-1195.

Sklar, L. S. and Dietrich, W. E. (2004). A mechanistic model for river incision into bedrock by saltating bed load. *Water Resources Research*, 40, 1-21.

Terzaghi, K. (1942). *Theoretical Soil Mechanics*. New York, NY: John Wiley and Sons, Inc.

Tinkler, K. and Wohl, E. (1998). A primer on bedrock channels. In *Rivers Over Rock: Fluvial Processes in Bedrock Channels (pp. 1-18).*

Turowski, J. M, Hovius, N., Wilson, A., and Horng, M.-J. (2007). Hydraulic geometry, river sediment and the definition of bedrock channels. *Geomorphology*, 99, 26-38.

APPENDIX I

Moisture Content Determination

Sample Number: 1

Date Tested: February 28, 2014

Tested by: Leila Pike

Weight of measuring tin, W1 (g)	183.8
Weight of measuring tin + moist soil, W2 (g)	437.1
Weight of measuring tin + dry soil, W3 (g)	412.2

$$MC(\%) = \frac{W2 - W3}{W3 - W1} * 100 = \frac{437.1 - 412.2}{412.2 - 183.8} * 100 = 10.9\%$$

Sample Number: 2

Date Tested: March 5, 2014

Tested by: Leila Pike

Weight of measuring tin, W1 (g)	175.6
Weight of measuring tin + moist soil, W2 (g)	446.6
Weight of measuring tin + dry soil, W3 (g)	420.1

$$MC(\%) = \frac{W2 - W3}{W3 - W1} * 100 = \frac{446.6 - 420.1}{420.1 - 175.6} * 100 = 10.8\%$$

Sample Number: 3

Date Tested: March 7, 2014

Tested by: Leila Pike

Weight of measuring tin, W1 (g)	175.6
Weight of measuring tin + moist soil, W2 (g)	372.2
Weight of measuring tin + dry soil, W3 (g)	333.8

$$MC(\%) = \frac{W2 - W3}{W3 - W1} * 100 = \frac{372.3 - 333.8}{333.8 - 175.6} * 100 = 24.3\%$$

Sample Number: 4

Date Tested: March 12, 2014

Tested by: Leila Pike

Weight of measuring tin, W1 (g)	175.6
Weight of measuring tin + moist soil, W2 (g)	328.4
Weight of measuring tin + dry soil, W3 (g)	299.6

$$MC(\%) = \frac{W2 - W3}{W3 - W1} * 100 = \frac{328.4 - 299.6}{299.6 - 175.6} * 100 = 23.2\%$$

Sample Number: 5

Date Tested: March 25, 2014

Tested by: Leila Pike

Weight of measuring tin, W1 (g)	183.9
Weight of measuring tin + moist soil, W2 (g)	497.9
Weight of measuring tin + dry soil, W3 (g)	466.5

$$MC(\%) = \frac{W2 - W3}{W3 - W1} * 100 = \frac{497.9 - 466.5}{466.5 - 183.9} * 100 = 11.1\%$$

Sample Number: 6

Date Tested: April 11, 2014

Tested by: Leila Pike

Weight of measuring tin, W1 (g)	183.6
Weight of measuring tin + moist soil, W2 (g)	454.9
Weight of measuring tin + dry soil, W3 (g)	426.3

$$MC(\%) = \frac{W2 - W3}{W3 - W1} * 100 = \frac{454.9 - 426.3}{426.3 - 183.6} * 100 = 11.8\%$$

APPENDIX II

Bulk Unit Weight Determination

Sample number: 1

Date tested: March 3, 2014

Tested by: Leila Pike

Mass of dry beaker, M1 (g)	271.3
Mass of beaker and air-dried sample, M2 (g)	524.0
Volume of water in beaker, V1 (mL)	500
Volume of water and sample in beaker, V2 (mL)	595

$$\gamma_d = \frac{(M_2 - M_1)g}{V} = \frac{(524.0 - 271.3) * 9.81}{95} = 26.1\,\frac{kN}{m^3}$$

Sample number: 2

Date tested: March 6, 2014

Tested by: Leila Pike

Mass of dry beaker, M1 (g)	271.3
Mass of beaker and air-dried sample, M2 (g)	514.8
Volume of water in beaker, V1 (mL)	400
Volume of water and sample in beaker, V2 (mL)	495

$$\gamma_d = \frac{(M_2 - M_1)g}{V} = \frac{(514.8 - 271.3) * 9.81}{95} = 25.1\,\frac{kN}{m^3}$$

Sample number: 3

Date tested: March 10, 2014

Tested by: Leila Pike

Mass of dry beaker, M1 (g)	271.3
Mass of beaker and air-dried sample, M2 (g)	510.9
Volume of water in beaker, V1 (mL)	500
Volume of water and sample in beaker, V2 (mL)	590

$$\gamma_d = \frac{(M_2 - M_1)g}{V} = \frac{(510.9 - 271.3) * 9.81}{90} = 26.1\,\frac{kN}{m^3}$$

Sample number: 4

Date tested: April 22, 2014

Tested by: Leila Pike

Mass of dry beaker, M1 (g)	271.3
Mass of beaker and air-dried sample, M2 (g)	520.9
Volume of water in beaker, V1 (mL)	450
Volume of water and sample in beaker, V2 (mL)	550

$$\gamma_d = \frac{(M_2 - M_1)g}{V} = \frac{(520.9 - 271.3) * 9.81}{105} = 24.5\,\frac{kN}{m^3}$$

Sample number: 5

Date tested: April 22, 2014

Tested by: Leila Pike

Mass of dry beaker, M1 (g)	271.3
Mass of beaker and air-dried sample, M2 (g)	500.2
Volume of water in beaker, V1 (mL)	450
Volume of water and sample in beaker, V2 (mL)	550

$$\gamma_d = \frac{(M_2 - M_1)g}{V} = \frac{(500.2 - 271.3) * 9.81}{90} = 25.0\,\frac{kN}{m^3}$$

Sample number: 6

Date tested: May 2, 2014

Tested by: Leila Pike

Mass of dry beaker, M1 (g)	284.6
Mass of beaker and air-dried sample, M2 (g)	467.4
Volume of water in beaker, V1 (mL)	350
Volume of water and sample in beaker, V2 (mL)	420

$$\gamma_d = \frac{(M_2 - M_1)g}{V} = \frac{(467.4 - 284.6) * 9.81}{70} = 25.6\,\frac{kN}{m^3}$$

APPENDIX III

Specific Gravity Determination

Sample number: 1

Date Tested: March 3, 2014

Tested by: Leila Pike

Mass of flask, Mf (g)	200.6
Mass of flask and water, Mfw (g)	684.8
Temperature of Water, T1 (*c)	21.8
Mass of sample, Ms (g)	169.0
Mass of flask with sample and water, Mfs (g)	780.6
Temperature of Water, T2 (*c)	21.8

$$G_s = \frac{M_s}{M_s + M_{fw} - M_{fs}} = \frac{169.0}{169.0 + 684.8 - 780.6} = 2.31$$

Sample number: 2

Date Tested: March 6, 2014

Tested by: Leila Pike

Mass of flask, Mf (g)	200.6
Mass of flask and water, Mfw (g)	684.3
Temperature of Water, T1 (*c)	21.9
Mass of sample, Ms (g)	117.3
Mass of flask with sample and water, Mfs (g)	751.3
Temperature of Water, T2 (*c)	21.9

$$G_s = \frac{M_s}{M_s + M_{fw} - M_{fs}} = \frac{117.3}{117.3 + 684.3 - 751.3} = 2.33$$

Sample number: 3

Date Tested: March 10, 2014

Tested by: Leila Pike

Mass of flask, Mf (g)	201.2
Mass of flask and water, Mfw (g)	679.6
Temperature of Water, T1 (*c)	21.8
Mass of sample, Ms (g)	181.9
Mass of flask with sample and water, Mfs (g)	787.9
Temperature of Water, T2 (*c)	21.8

$$G_s = \frac{M_s}{M_s + M_{fw} - M_{fs}} = \frac{181.9}{181.9 + 679.6 - 787.9} = 2.47$$

Sample number: 4

Date Tested: April 22, 2014

Tested by: Leila Pike

Mass of flask, Mf (g)	200.5
Mass of flask and water, Mfw (g)	682.4
Temperature of Water, T1 (*C)	25.9
Mass of sample, Ms (g)	160.4
Mass of flask with sample and water, Mfs (g)	773.0
Temperature of Water, T2 (*C)	25.9

$$G_s = \frac{M_s}{M_s + M_{fw} - M_{fs}} = \frac{160.4}{160.4 + 682.4 - 773.0} = 2.30$$

Sample number: 5

Date Tested: April 22, 2014

Tested by: Leila Pike

Mass of flask, Mf (g)	201.2
Mass of flask and water, Mfw (g)	680.3
Temperature of Water, T1 (*C)	26.0
Mass of sample, Ms (g)	188.7
Mass of flask with sample and water, Mfs (g)	788.0
Temperature of Water, T2 (*C)	26.0

$$G_s = \frac{M_s}{M_s + M_{fw} - M_{fs}} = \frac{188.7}{188.7 + 680.3 - 788.0} = 2.33$$

Sample number: 6

Date Tested: May 2, 2014

Tested by: Leila Pike

Mass of flask, Mf (g)	201.2
Mass of flask and water, Mfw (g)	681.3
Temperature of Water, T1 (*C)	26.0
Mass of sample, Ms (g)	115.7
Mass of flask with sample and water, Mfs (g)	749.3
Temperature of Water, T2 (*C)	26.0

$$G_s = \frac{M_s}{M_s + M_{fw} - M_{fs}} = \frac{115.7}{115.7 + 681.1 - 749.3} = 2.44$$

APPENDIX IV

Particle Size Distribution Tests

Sample 1

Weight of dry sample: 733.97 g

Sieve Analysis:

Sieve Number	Size (mm)	Soil Retained (g)	Mass Percent (%)	Cumulative Mass Percent (%)	Percent Passing (%)
4	4.75	23.78	3.24	3.24	96.76
14	1.4	4.27	0.58	3.82	96.18
30	0.599	42.68	5.81	9.64	90.36
60	0.251	30.44	4.15	13.78	86.22
120	0.125	14.03	1.91	15.70	84.30
140	0.104	31.57	4.30	20.00	80.00
200	0.075	45.1	6.14	26.14	73.86
Pan	-	538.53	73.37	99.51	0.49
	Total:	730.40			

Hydrometer Analysis:

M1: 50.01 g
Co: 0
Cm: 1
Temp: 25.5℃

Time elapsed (min.)	Hydrometer Reading	Temperature (℃)	Hydrometer Reading with Meniscus Correction	Effective Hydrometer Depth, L (cm)	K	Equivalent Particle Diameter, D (mm)	Temperature Correction, Ct	a	Corrected Hydrometer Reading, Rc	Percent Finer (%)	Adjusted Percent Finer (%)
0											
1	43.5	25.5	44.5	9	0.01342	0.04026	1.475	0.995	44.98	89.48	66.09
2	40	25.5	41	9.6	0.01342	0.02940	1.475	0.995	41.48	82.52	60.95
4	37	25.5	38	10.1	0.01342	0.02132	1.475	0.995	38.48	76.55	56.54
8	34	25.5	35	10.6	0.01342	0.01545	1.475	0.995	35.48	70.58	52.13
16	30	25.5	31	11.2	0.01342	0.01123	1.475	0.995	31.48	62.62	46.25
30	27	25.5	28	11.7	0.01342	0.00838	1.475	0.995	28.48	56.65	41.84
120	21	26	22	12.7	0.01334	0.00434	1.65	0.995	22.65	45.06	33.28
1440	13	26	14	14	0.01334	0.00132	1.65	0.995	14.65	29.15	21.53

Sample 2

Weight of dry sample:668.00 g

Sieve Analysis:

Sieve Number	Size (mm)	Soil Retained (g)	Mass Percent (%)	Cumulative Mass Percent (%)	Percent Passing (%)
4	4.75	33.1	4.96	4.96	95.04
8	2.36	17	2.54	7.50	92.50
16	1.18	15.4	2.31	9.81	90.19
30	0.6	14	2.10	11.90	88.10
60	0.25	34.8	5.21	17.11	82.89
120	0.125	36.9	5.52	22.63	77.37
140	0.106	11.3	1.69	24.33	75.67
200	0.075	18.8	2.81	27.14	72.86
pan	-	486.7	72.86	100.00	0.00
	Total	668			

Hydrometer Analysis:

M1: 50.00 g
Co: -2.2
Cm: 1.2
Temp: 24.0 ℃

Time elapsed (min.)	Hydrometer Reading	Temperature (℃)	Hydrometer Reading with Meniscus Correction	Effective Hydrometer Depth, L (cm)	K	Equivalent Particle Diameter, D (mm)	Temperature Correction, Ct	a	Corrected Hydrometer Reading, Rc	Percent Finer (%)	Adjusted Percent Finer (%)
0											
1	38.5	24	41.85	9.76	0.009541	0.02981	1.15	1.091	39.7	91.29	66.52
2	37	24	40.35	10.06	0.009541	0.02140	1.15	1.091	38.2	88.02	64.13
4	35	24	38.35	10.36	0.009541	0.01535	1.15	1.091	36.2	83.66	60.95
8	33	24	36.35	10.66	0.009541	0.01101	1.15	1.091	34.2	79.30	57.77
16	31	24	34.35	11.06	0.009541	0.00793	1.15	1.091	32.2	74.93	54.60
30	28	24	31.35	11.46	0.009541	0.00590	1.15	1.091	29.2	68.39	49.83
120	22	24	25.35	12.46	0.009541	0.00307	1.15	1.091	23.2	55.30	40.29
1440	13	24	16.35	13.96	0.009541	0.00094	1.15	1.091	14.2	35.67	25.99

Sample 4

Weight of dry sample: 611.30 g

Sieve Analysis:

Sieve Number	Size (mm)	Soil Retained (g)	Mass Percent (%)	Cumulative Mass Percent (%)	Percent Passing (%)
4	4.75	31.9	5.22	5.22	94.78
8	2.36	14.6	2.39	7.61	92.39
16	1.18	14	2.29	9.90	90.10
30	0.6	15.3	2.50	12.40	87.60
60	0.25	28.1	4.60	17.00	83.00
120	0.125	29	4.74	21.74	78.26
140	0.106	7.2	1.18	22.92	77.08
200	0.075	18.3	2.99	25.91	74.09
pan	-	452.9	74.09	100.00	0.00
	Total	611.3			

Hydrometer Analysis:

M1: 50.00 g
Co: 24
Cm: 1.1
Temp: 24.0℃

Time elapsed (min.)	Hydrometer Reading	Temperature (℃)	Hydrometer Reading with Meniscus Correction	Effective Hydrometer Depth, L (cm)	K	Equivalent Particle Diameter, D (mm)	Temperature Correction, Ct	a	Corrected Hydrometer Reading, Rc	Percent Finer (%)	Adjusted Percent Finer (%)
0											
1	65	24	42.15	9.38	0.00954	0.02922	1.15	1.091	66.1	91.95	68.12
2	63	24	40.15	9.71	0.00954	0.02102	1.15	1.091	64.1	87.58	64.89
4	61	24	38.15	10.04	0.00954	0.01511	1.15	1.091	62.1	83.22	61.66
8	58.5	23.5	35.525	10.47	0.00961	0.01100	1.025	1.091	59.6	77.50	57.42
16	55.5	23.5	32.525	10.96	0.00961	0.00796	1.025	1.091	56.6	70.95	52.57
30	52.5	23.5	29.525	11.46	0.00961	0.00594	1.025	1.091	53.6	64.41	47.72
120	46	24	23.15	12.46	0.00954	0.00307	1.15	1.091	47.1	50.50	37.41
1440	36	25	13.4	13.96	0.00940	0.00093	1.4	1.091	37.1	29.23	21.66

APPENDIX V

Alluvial Cover Particle Size Distribution

Length of Axis a (cm)	Length of Axis b (cm)	Length of Axis c (cm)	Diameter (cm)	Volume (cm^3)	Weight (assuming specific gravity is 2.65) g	Mass Percent (%)	Cum. Mass Percent (%)	Percent Passing (%)
7	4.5	1.5	3.74	27.43	72.68	8.43	8.43	91.57
4.5	3.1	1.1	3.40	20.50	54.32	6.30	14.73	85.27
6.5	4.6	1.7	3.22	17.42	46.17	5.35	20.08	79.92
8.3	7.7	2.5	3.20	17.12	45.37	5.26	25.34	74.66
3	2.5	0.9	3.04	14.75	39.09	4.53	29.87	70.13
6.9	6	2.3	2.80	11.46	30.38	3.52	33.39	66.61
6.9	4.2	2.1	2.56	8.82	23.37	2.71	36.10	63.90
9.5	5	2.8	2.46	7.81	20.69	2.40	38.50	61.50
4.8	3.6	1.7	2.45	7.66	20.29	2.35	40.86	59.14
2.9	2	1	2.41	7.31	19.38	2.25	43.10	56.90
7	6.8	2.9	2.38	7.05	18.68	2.17	45.27	54.73
4.2	3.3	1.6	2.33	6.60	17.48	2.03	47.30	52.70
5.5	3.5	1.9	2.31	6.45	17.09	1.98	49.28	50.72
8.7	5.5	3	2.31	6.42	17.01	1.97	51.25	48.75
5.4	5	2.3	2.26	6.04	16.00	1.86	53.10	46.90
2.1	1.9	0.9	2.22	5.72	15.17	1.76	54.86	45.14
7.3	6	3	2.21	5.62	14.90	1.73	56.59	43.41
6.5	4.6	2.5	2.19	5.48	14.52	1.68	58.27	41.73
7	4.9	2.7	2.17	5.34	14.16	1.64	59.92	40.08
3.9	2.6	1.5	2.12	5.01	13.27	1.54	61.46	38.54
5	4.2	2.2	2.08	4.73	12.54	1.45	62.91	37.09
7.7	6.3	3.4	2.05	4.50	11.93	1.38	64.29	35.71
5.4	3.5	2.2	1.98	4.04	10.71	1.24	65.53	34.47
4.2	3	1.8	1.97	4.02	10.64	1.23	66.77	33.23
3.6	3.4	1.8	1.94	3.84	10.19	1.18	67.95	32.05
5.3	4.4	2.5	1.93	3.77	10.00	1.16	69.11	30.89
3.4	3.1	1.7	1.91	3.65	9.66	1.12	70.23	29.77
5.6	4.5	2.7	1.86	3.37	8.92	1.03	71.26	28.74
7	4.4	3	1.85	3.31	8.78	1.02	72.28	27.72
7.3	5	3.3	1.83	3.21	8.51	0.99	73.27	26.73
4.7	4.3	2.5	1.80	3.04	8.07	0.94	74.20	25.80
5.4	5	2.9	1.79	3.01	7.98	0.93	75.13	24.87
3.6	3.2	1.9	1.79	2.98	7.91	0.92	76.05	23.95
5.8	3.9	2.7	1.76	2.86	7.58	0.88	76.93	23.07
4.5	4.3	2.5	1.76	2.85	7.56	0.88	77.80	22.20
4	3.3	2.1	1.73	2.71	7.19	0.83	78.64	21.36
4.5	3.7	2.4	1.70	2.57	6.82	0.79	79.43	20.57
5.5	3.8	2.7	1.69	2.54	6.74	0.78	80.21	19.79
7.5	7.3	4.4	1.68	2.49	6.60	0.77	80.97	19.03
5.6	3.3	2.6	1.65	2.37	6.27	0.73	81.70	18.30
7.7	5.5	4	1.63	2.25	5.98	0.69	82.39	17.61
6.2	5.5	3.6	1.62	2.23	5.92	0.69	83.08	16.92
4.7	4	2.7	1.61	2.17	5.75	0.67	83.75	16.25
4.8	4.5	2.9	1.60	2.16	5.71	0.66	84.41	15.59
6	5.2	3.5	1.60	2.13	5.64	0.65	85.06	14.94
4.5	3.5	2.5	1.59	2.09	5.55	0.64	85.70	14.30
4.4	3.8	2.6	1.57	2.04	5.40	0.63	86.33	13.67
3.2	2.5	1.8	1.57	2.03	5.38	0.62	86.95	13.05
3.9	2.5	2	1.56	1.99	5.28	0.61	87.57	12.43

Length of Axis a (cm)	Length of Axis b (cm)	Length of Axis c (cm)	Diameter (cm)	Volume (cm^3)	Weight (assuming specific gravity is 2.65) g	Mass Percent (%)	Cum. Mass Percent (%)	Percent Passing (%)
3.4	2.5	1.9	1.53	1.89	5.01	0.58	88.15	11.85
5.7	3.7	3	1.53	1.88	4.98	0.58	88.73	11.27
2.8	2.7	1.8	1.53	1.87	4.95	0.57	89.30	10.70
4.9	4.5	3.1	1.51	1.82	4.82	0.56	89.86	10.14
5	4.1	3	1.51	1.80	4.77	0.55	90.41	9.59
5.5	4.2	3.2	1.50	1.77	4.70	0.55	90.96	9.04
3.5	1.8	1.7	1.48	1.69	4.47	0.52	91.47	8.53
3.9	3.2	2.4	1.47	1.67	4.43	0.51	91.99	8.01
6.2	4.2	3.5	1.46	1.62	4.30	0.50	92.49	7.51
5.5	2.6	2.6	1.45	1.61	4.27	0.49	92.98	7.02
4.5	3.8	2.9	1.43	1.52	4.02	0.47	93.45	6.55
3	2.7	2	1.42	1.51	4.00	0.46	93.91	6.09
3.5	2.8	2.2	1.42	1.51	4.00	0.46	94.37	5.63
6	4.1	3.5	1.42	1.49	3.95	0.46	94.83	5.17
3	1.7	1.6	1.41	1.47	3.90	0.45	95.28	4.72
7	5	4.2	1.41	1.46	3.88	0.45	95.73	4.27
7	4.7	4.1	1.40	1.43	3.80	0.44	96.17	3.83
3.4	3.3	2.4	1.40	1.42	3.77	0.44	96.61	3.39
3.9	2.9	2.5	1.35	1.27	3.38	0.39	97.00	3.00
5.9	4.2	3.8	1.31	1.18	3.12	0.36	97.37	2.63
3.6	2.3	2.2	1.31	1.17	3.10	0.36	97.73	2.27
5.2	3.1	3.1	1.30	1.14	3.01	0.35	98.07	1.93
5.6	4.3	3.8	1.29	1.13	2.99	0.35	98.42	1.58
6.2	4.7	4.2	1.29	1.11	2.95	0.34	98.76	1.24
5.6	4.6	4.1	1.24	0.99	2.63	0.31	99.07	0.93
4.8	3.2	3.2	1.22	0.96	2.55	0.30	99.36	0.64
5.8	4.7	4.5	1.16	0.82	2.17	0.25	99.61	0.39
5.1	4.7	4.6	1.06	0.63	1.67	0.19	99.81	0.19
5.5	5.1	5	1.06	0.62	1.65	0.19	100.00	0.00
				Total	862.46			

APPENDIX VI

Hydraulic Flume Test Measurements and Notes

Sample 1 Flume Test:

Slope, S	Flow, Q (gpm)	Flow, Q (m^3/s)	Depth, y (cm)	Velocity, V (m/s)	Fr	Hydraulic Radius, R (m)	Shear Stress, τ_o (Pa)	Error (+/-) (Pa)	Start Time	End Time	Duration (hrs)	Observations
0.031	23	0.0015	0.42	0.86	4.26	0.004114	1.3	0.8	13:45	14:15	0.5	smoothing of the surface
0.031	40	0.0025	0.65	0.97	3.84	0.006295	1.9	0.5	14:15	14:45	0.5	nothing more happening
0.031	67	0.0042	1	1.06	3.37	0.009524	2.9	0.8	14:45	15:00	0.25	nothing more happening
0.031	82	0.0052	1.15	1.12	3.35	0.010875	3.3	0.5	15:00	15:15	0.25	nothing more happening
0.031	97	0.0061	1.3	1.18	3.30	0.012207	3.7	0.6	15:15	14:30	0.25	nothing more happening
0.031	110	0.0069	1.4	1.24	3.34	0.013084	4.0	0.5	15:30	15:45	0.25	nothing more happening
0.031	130	0.0082	1.61	1.27	3.20	0.014901	4.5	0.7	15:45	16:00	0.25	nothing more happening
0.031	157	0.0099	1.86	1.33	3.12	0.017017	5.2	0.8	16:00	16:30	0.5	nothing more happening
0.031	172	0.0109	2.01	1.35	3.04	0.018264	5.6	0.7	16:30	16:45	0.25	nothing more happening
0.031	186	0.0117	2.16	1.36	2.95	0.019495	5.9	0.7	16:45	17:00	0.25	nothing more happening
0.031	205	0.0129	2.29	1.41	2.98	0.020547	6.2	0.7	17:00	17:30	0.5	nothing more happening
0.031	213	0.0134	2.49	1.35	2.73	0.022143	6.7	0.8	17:30	18:00	0.5	crack down middle
0.035	213	0.0134	2.2	1.53	3.29	0.01982	6.8	0.6	10:45	11:00	0.25	nothing extra
0.036	215	0.0136	2.17	1.56	3.39	0.019576	6.9	0.7	11:00	11:30	0.5	chunk fell off already damaged corner
0.039	215	0.0136	2.1	1.61	3.56	0.019005	7.3	0.8	11:30	12:15	0.75	nothing more happening
0.044	215	0.0136	2.02	1.68	3.77	0.018347	7.9	1.0	12:15	17:00	4.75	corner chunk falls off, crack is enlarging, chunks dislodging from crack
0.046	215	0.0136	2	1.70	3.83	0.018182	8.2	0.9	11:15	13:15	2	pink rock becoming more visible along edge - surface erosion
									Total Time:		12.5	

Sample 2 Flume Test:

Slope, S	Flow, Q (gpm)	Flow, Q (m^3/s)	Depth, y (cm)	Velocity, V (m/s)	Fr	Hydraulic Radius, R (m)	Shear Stress, τ_o (Pa)	Error (+/-) (Pa)	Start Time	End Time	Duration (hrs)	Observations
0.046	18	0.0011	0.39	0.73	3.72	0.003825	1.7	1.1	10:00	10:15	0.25	corner erosion and damage
0.046	37	0.0023	0.63	0.93	3.73	0.006108	2.8	0.8	10:15	10:30	0.25	the other corner chipped off, some smoothing
0.046	51	0.0032	0.75	1.07	3.95	0.007229	3.3	0.6	10:30	10:45	0.25	edge pieces cracking
0.046	82	0.0052	0.98	1.32	4.26	0.009342	4.2	0.9	10:45	11:00	0.25	smoothing
0.046	104	0.0066	1.21	1.36	3.93	0.01141	5.1	1.0	11:00	11:30	0.5	nothing extra
0.046	132	0.0083	1.45	1.44	3.81	0.01352	6.1	1.0	11:30	12:00	0.5	nothing extra
0.046	156	0.0098	1.6	1.54	3.88	0.014815	6.7	0.9	12:00	13:15	1.25	very small gravel pieces popping out of surface
0.046	181	0.0114	1.74	1.64	3.97	0.016007	7.2	0.9	13:15	14:15	1	large edge and corner piece breaking off
0.046	195	0.0123	1.84	1.67	3.93	0.01685	7.6	0.9	14:15	15:15	1	small cracks forming around edges, crack forming from gravel piece to edge of sample
0.046	204	0.0129	1.92	1.68	3.86	0.017518	7.9	0.9	15:15	16:15	1	more cracks forming
0.046	210	0.0132	2.02	1.64	3.68	0.018347	8.3	0.9	16:15	17:15	1	scouring in cracks, pitting, more cracks forming around gravel pieces, small gravel pieces popping out, chunks falling out of cracks
0.046	210	0.0132	2.02	1.64	3.68	0.018347	8.3	0.7	9:00	10:00	1	nothing extra
0.046	215	0.0136	2.1	1.61	3.56	0.019005	8.6	0.9	10:00	13:00	3	enlargening cracks, edge falling off
0.046	218	0.0138	2.15	1.60	3.48	0.019413	8.8	0.9	13:00	16:30	3	crack forming on upstream side of gravel piece, upstream corner fell off, large crack formed crossing over the sample
									Total Time:		14.25	

Sample 3 Flume Test:

Slope, S	Flow, Q (gpm)	Flow, Q (m^3/s)	Depth, y (cm)	Velocity, V (m/s)	Fr	Hydraulic Radius, R (m)	Shear Stress, τ_o (Pa)	Error (+/-) (Pa)	Start Time	End Time	Duration (hrs)	Observations
0.046	18	0.001136	0.28	1.01	6.12	0.002761	1.2	0.8	9:00	9:30	0.5	Major mass erosion, small chunks, sample loses structure and slumps

Sample 4 Flume Test:

Slope, S	Flow, Q (gpm)	Flow, Q (m^3/s)	Depth, y (cm)	Velocity, V (m/s)	Fr	Hydraulic Radius, R (m)	Shear Stress, τ_o (Pa)	Error (+/-) (Pa)	Start Time	End Time	Duration (hrs)	Observations
0.046	18	0.001136	0.2	1.42	10.13	0.00198	0.9	0.6	10:00	11:00	1	Dislodged loose particles on top, eroding around gravel pieces, "flocs" of clay particles eroding – mass erosion, gravel pieces remaining on top, integrity seems to be higher than sample 3

Sample 5 Flume Tests:

Slope, S	Flow, Q (gpm)	Flow, Q (m^3/s)	Depth, y (cm)	Velocity, V (m/s)	Fr	Hydraulic Radius, R (m)	Shear Stress, τ_o (Pa)	Error (+/-) (Pa)	Start Time	End Time	Duration (hrs)	Observations
0.046	16	0.0010	0.32	0.79	4.45	0.00315	1.4	0.9	11:15	11:45	0.5	alluvial cover stationary upstream, no erosion on sample
0.046	26	0.0016	1.01	0.41	1.29	0.009614	4.3	1.9	11:45	12:00	0.25	alluvial cover moving slowly, local eddy effects on sample, no erosion
0.046	84	0.0053	2.15	0.62	1.34	0.019413	8.8	3.0	12:00	12:30	0.5	localized subcritical flow - some alluvial cover rolling over sample, and then remaining stationary, sample almost fully covered
0.046	104	0.0066	2.35	0.70	1.45	0.021029	9.5	1.2	12:30	13:30	1	sliding alluvial cover causes corner damage - cover stays stationary - subcritical flow around sample
0.046	138	0.0087	1.62	1.34	3.37	0.014986	6.8	0.7	13:30	14:30	1	corner damage - alluvial cover rolling quickly, no longer subcritical flow where sample is, surface pitting, some small cracks forming
0.046	162	0.0102	1.7	1.50	3.68	0.015668	7.1	0.8	14:30	15:45	1.25	center gravel pieces dislodge
0.046	186	0.0117	1.82	1.61	3.81	0.016682	7.5	0.9	15:45	17:00	1.25	gravel coming out the center and damage around the edges
0.046	186	0.0117	1.94	1.51	3.47	0.017685	8.0	0.9	9:30	11:30	2	edge piece fell off, side cracking, mass erosion occurring from damaged areas, crack across sample, gravel causes cracks to enlarge at a fast pace, areas delineating and dislodging – Very noticeable increase in incision / smoothing of surface
0.046	197	0.0124	2.01	1.55	3.48	0.018264	8.2	0.9	11:30	12:15	0.75	mass erosion
0.046	205	0.0129	2.17	1.49	3.23	0.019576	8.8	1.1	12:15	16:00	3.75	continued incision, mass erosion, upward edge eroding
									Total Time:		12.25	

Sample 6 Flume Tests:

Slope, S	Flow, Q (gpm)	Flow, Q (m^3/s)	Depth, y (cm)	Velocity, V (m/s)	Fr	Hydraulic Radius, R (m)	Shear Stress, τ_o (Pa)	Error (+/-) (Pa	Start Time	End Time	Duration (hrs)	Observations
0.046	32	0.0020	1.23	0.41	1.18	0.011587	5.2	3.1	12:30	13:00	0.5	gravel stays upstream
0.046	51	0.0032	0.99	0.81	2.61	0.009433	4.3	-0.1	13:00	13:30	0.5	gravel rearranged itself a bit, changing depth of water over sample
0.046	71	0.0045	2	0.56	1.26	0.018182	8.2	2.7	13:30	14:00	0.5	Gravel moved, causing extra depth over sample, gravel moved to cover sample
0.046	100	0.0063	2.5	0.63	1.27	0.022222	10.0	1.8	14:00	17:00	3	Gravel cover slowly moved, some on sample, small divot in surface. Gravel on top of sample, erosion occurred while gravel on sample
0.046	133	0.0084	1.45-2.08	1.45-1.01	3.84-2.23	0.0135-0.0188	6.1-8.5	1.0	11:15	12:15	1	Gravel moved, but still some on sample, shear stress value is an estimate. When gravel moved, surface no longer flat and smooth
0.046	165	0.0104	1.73	1.50	3.65	0.015923	7.2	1.1	12:15	13:15	1	Gravel stationary on sample
0.046	184	0.0116	1.91	1.52	3.51	0.017435	7.9	0.9	13:15	14:15	1	Gravel rolling causes corner damage, mass erosion - cracks formed and gravel causes chunks to dislodge, cracks around gravel piece within sample, mass erosion
0.046	192	0.0121	1.99	1.52	3.44	0.018099	8.2	0.9	14:15	16:15	2	large chunks dislodged near cracked corner areas and from center
0.046	205	0.0129	2.08	1.55	3.44	0.018841	8.5	0.8	10:45	12:45	2	Gravel moving quickly, caused increased incision and smoothing
0.046	210	0.0132	2.11	1.57	3.45	0.019086	8.6	0.8	12:45	15:45	3	small gravel pieces dislodged from center of sample
									Total Time:		14.5	